Air Pollution
ENV-409

Multiphase equilibria

Multiphase equilibria

To understand the fate of compounds in the environment, we need to understand how they partition among the various available phases:

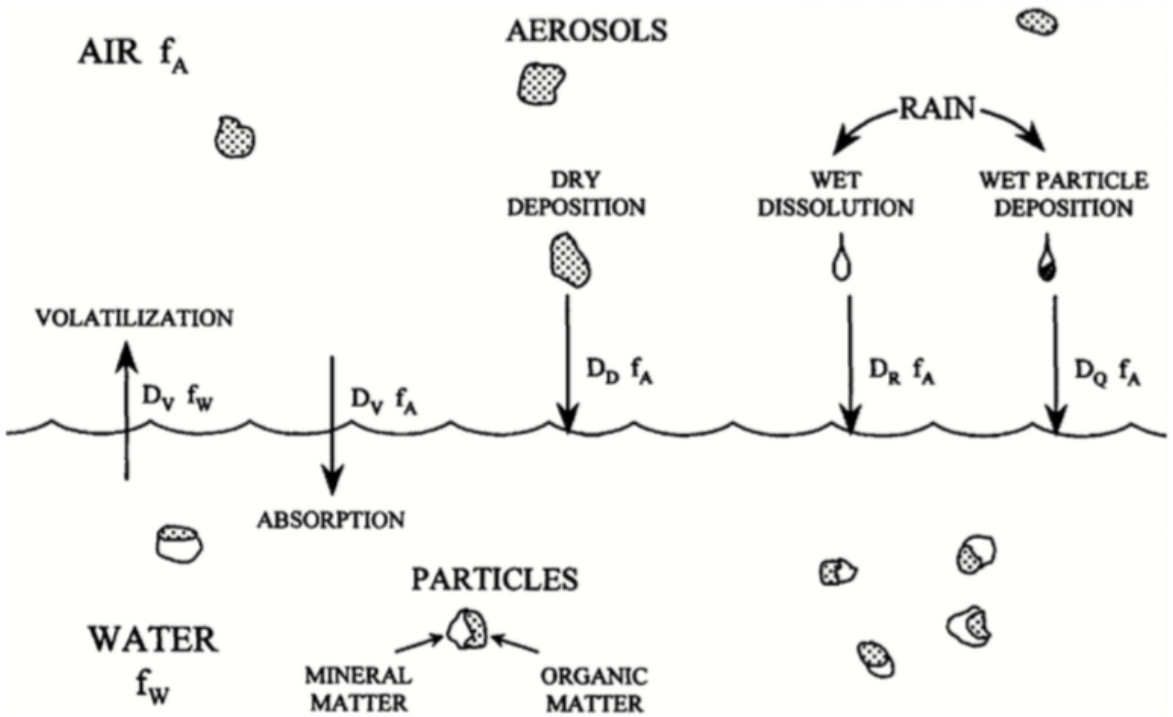

Mackay, 2001

Questions:

1. What phase do pure substances prefer to reside in?
2. How does this change with environmental conditions and mixture properties?

While thermodynamic concepts are applicable very generally, we will use them to look at gas/particle partitioning processes.

Aerosols

Particulate matter; aerosols are particles suspended in air.

Examples of aerosol classifications:

- nonvolatile/semi-volatile,
- primary/secondary
- anthropogenic/biogenic
- $PM_{2.5}/PM_{10}$/ultrafine
- spherical/non-spherical
- solid/liquid/mixed

Impacts:

- inhalation linked to adverse health effects
- cloud droplet formation (influences precipitation and global/local energy balance)

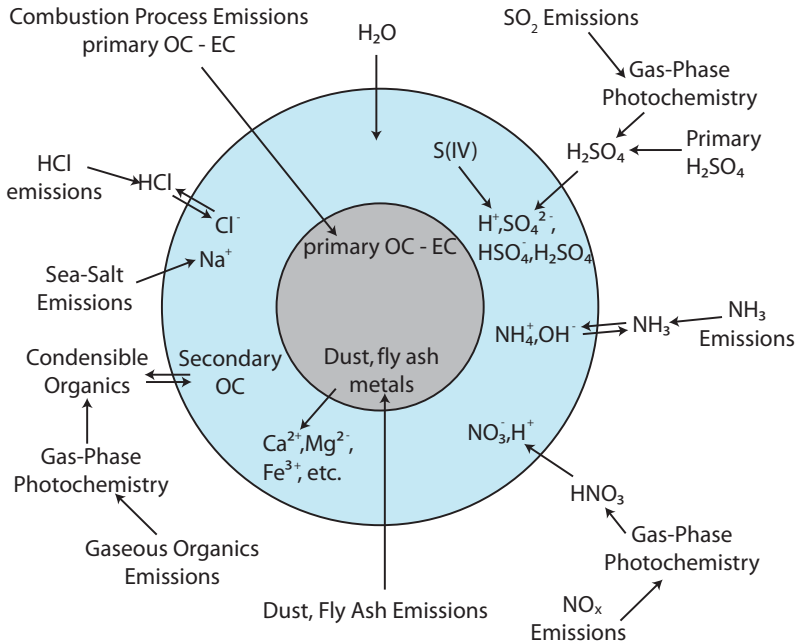

adapted from Pandis et al., 1995

PM_{10} mass concentrations

(2013 Switzerland)

Seasonal variations:

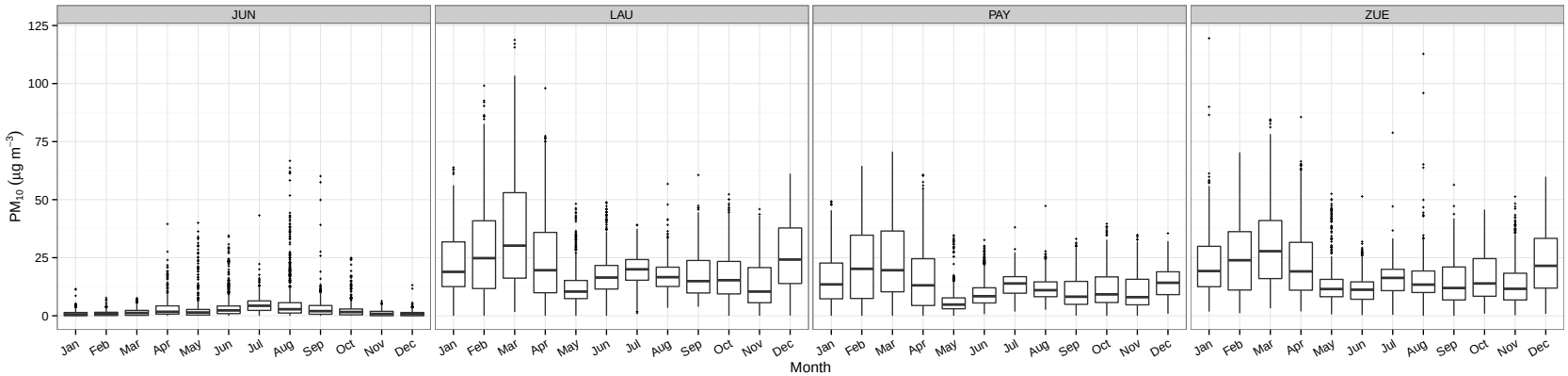

Diurnal variations:

PM$_1$ mass concentrations

(2011–2013 Paris)

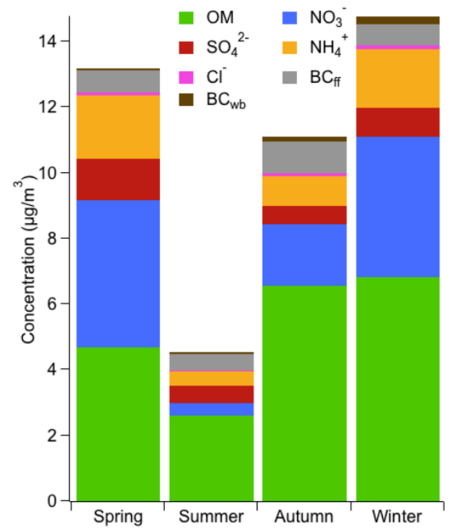

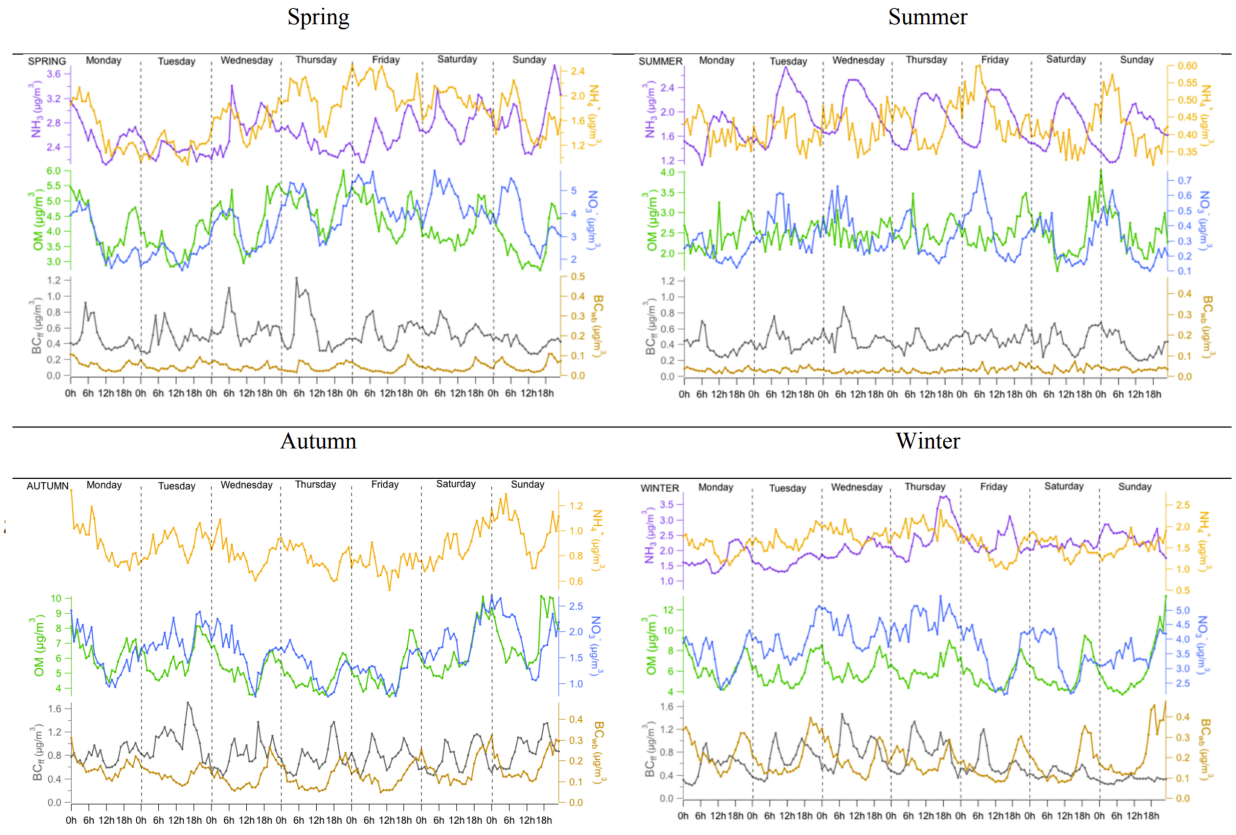

Petit et al., *Atmos. Chem. Phys.*, 2015

Atmospheric aerosols processes

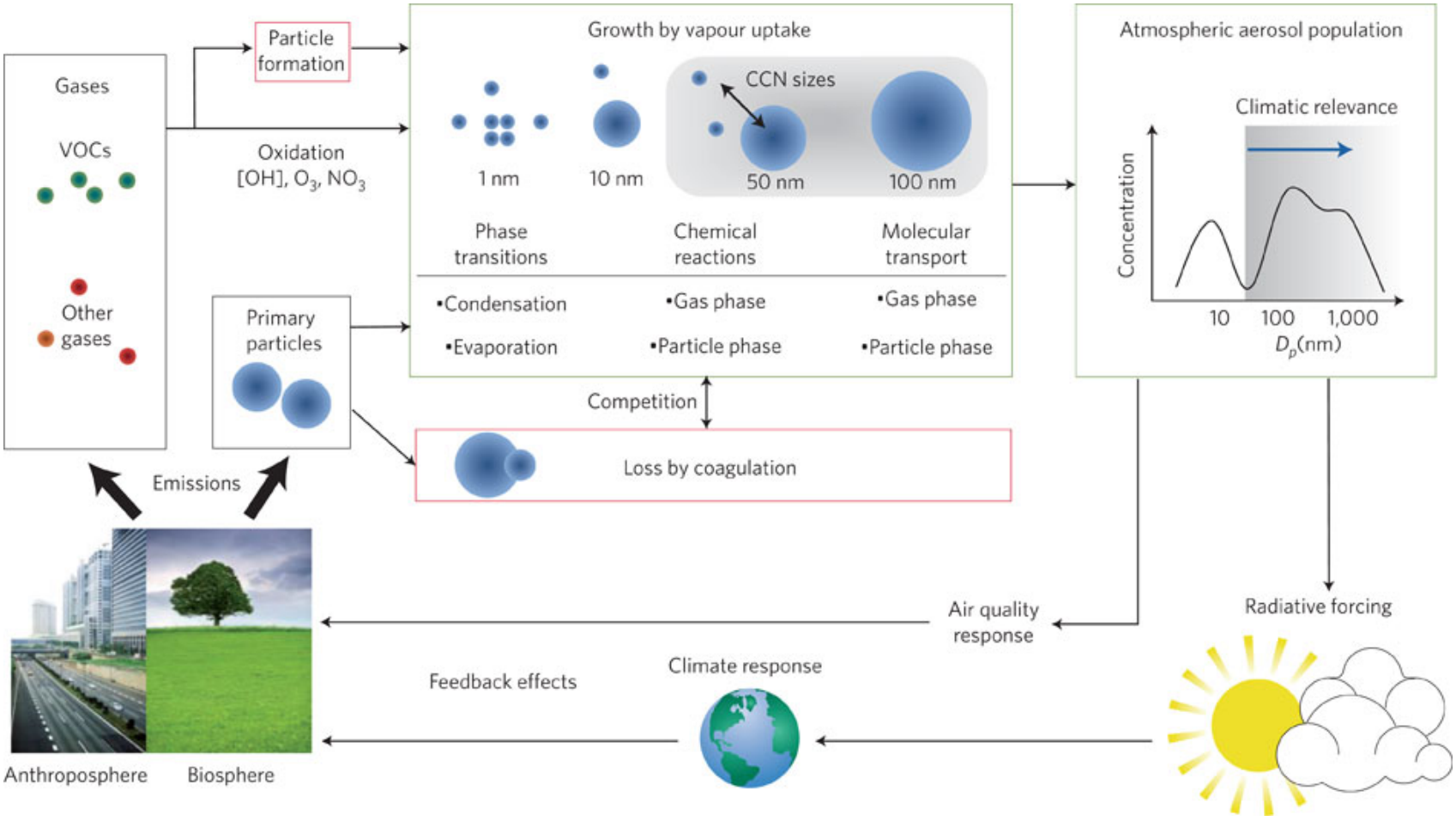

Riipinen et al., 2012

Gas/particle conversion mechanisms

Overview of mechanisms:

- **New particle formation**. Aerosols grow from molecular clusters formed in the gas phase by a process known as *nucleation* (formation of a new phase—i.e., particle from gas).
- **Gas/particle partitioning**. Gases converted into particles by *condensation* onto pre-existing aerosols.
  - surface adsorption
  - bulk absorption

We wish to describe models of gas/particle partitioning which allow us to predict the atmospheric state from a set of prescribed emissions or precursor concentrations.

Since aerosols affect the global/local energy balance and precipitation patterns, these predictions would hinge on our ability to accurately calculate aerosol burdens in space and time.

We focus on the second case (condensation/evaporation) in this lecture, as it is ubiquitous, energetically favorable, and regulates PM mass.

Example mechanisms: gas/particle partitioning of inorganic compounds

Some reactions among inorganic compounds which form condensible products. From Seinfeld and Pandis (2006) Table 10.7 and and Pilinis et al. (2000):

$$NH_{3(g)} + HNO_{3(g)} \rightleftharpoons NH_4NO_{3(s)}$$

$$NH_{3(g)} + HCl_{(g)} \rightleftharpoons NH_4Cl_{(s)}$$

$$NH_{3(g)} + HNO_{3(g)} \rightleftharpoons NH_4^+ + NO_3^-$$

$$NH_{3(g)} + HCl_{(g)} \rightleftharpoons NH_4^+ + Cl^-$$

$$H_2SO_{4(g)} \rightarrow H^+ + HSO_4^-$$

$$HNO_{3(g)} \rightleftharpoons H^+ + NO_3^-$$

$$HCl_{(g)} \rightleftharpoons H^+ + Cl^-$$

$$NaCl_{(s)} + HNO_{3(g)} \rightleftharpoons NaNO_{3(s)} + HCl_{(g)}$$

$$2NaCl_{(s)} + H_2SO_{4(g)} \rightarrow Na_2SO_{4(s)} + 2HCl_{(g)}$$

$$2NaNO_{3(s)} + H_2SO_{4(g)} \rightarrow Na_2SO_{4(s)} + 2HNO_{3(g)}$$

$$2NH_4NO_{3(s)} + H_2SO_{4(g)} \rightarrow (NH_4)_2SO_{4(s)} + 2HNO_{3(g)}$$

$$2NH_4Cl_{(s)} + H_2SO_{4(g)} \rightarrow (NH_4)_2SO_{4(s)} + 2HCl_{(g)}$$

$$NH_{3(g)} \rightleftharpoons NH_{3(aq)}$$

Note that sulfate species strongly favor the condensed phase.

Example framework: gas/particle partitioning of organic compounds

This is a rapidly changing field of research; the traditional viewpoint is presented here. Oxidation of a reactive organic gas (ROG) forms n condensible products (P) with stochiometric coefficients, a:

$$\mathrm{ROG} \overset{\text{Oxidant}}{\rightarrow} a_1 P_1 + a_2 P_2 + \ldots a_k P_k \ldots + a_n P_n$$

Each of these products can partition between the gas and particle phase:

$$P_{k,(\mathrm{g})} \rightleftharpoons P_{k,(\mathrm{l})} \; \forall \; k = \{1, 2, \ldots, n\}$$

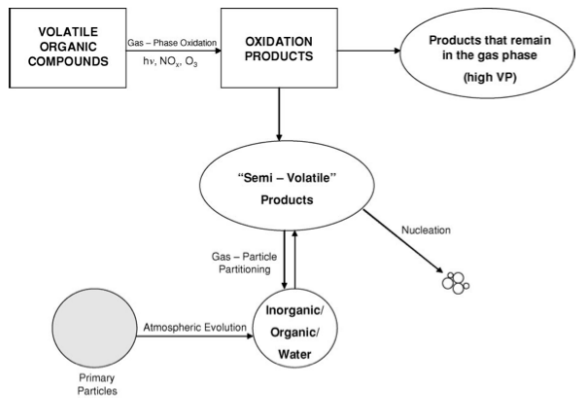

Figure 1 Route of formation of secondary organic particulate matter. Products of sufficiently low volatility, so-called "semi-volatile," may condense on pre-existing particles, which generally consist of inorganics, organics, and water, or nucleate homogeneously to form new particles.

Seinfeld and Pankow, 2003

A more modern view of secondary organic aerosol formation consideres multigeneration oxidation products — many of the products can undergo further oxidation reactions.

Multigenerational aging

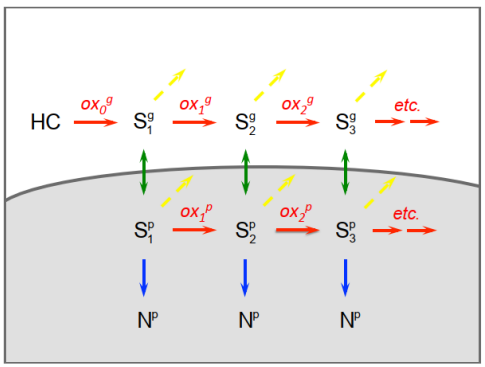

Fig. 1. Scheme for SOA formation and evolution, showing multigenerational gas- and particle-phase reactions, in the functional group oxidation model. "S" and "N" denote semivolatile and nonvolatile compounds, respectively. Note that the single product for each generation shown here represents a spectrum of products spanning a range of volatilities and oxidation states. The oxidation of semivolatile compounds comprises two processes: functionalization (red arrows) and fragmentation (yellow arrows). Instantaneous equilibrium partitioning is assumed (green arrows). Nonoxidative (accretion) reactions are considered as bimolecular irreversible reactions (blue arrows).

Zhang and Seinfeld, *Atmos. Chem. Phys.*, 2013

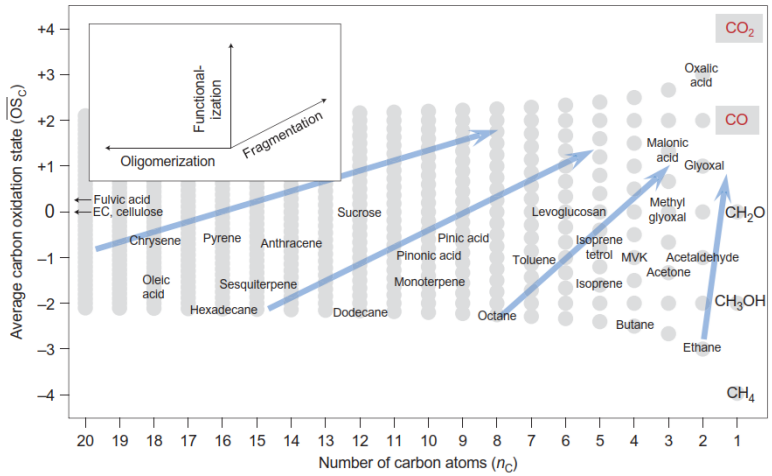

Figure 1 | Possible combinations of average carbon oxidation state ($\overline{OS}_C$) and number of carbon atoms (n_C) for stable organic molecules. Any organic species can be placed in this two-dimensional space; the locations of key atmospheric organics (and common surrogate species) are shown. The vast majority of known atmospheric species are reduced ($\overline{OS}_C \leq 0$), with only the smallest compounds having higher oxidation states. Inset: vectors corresponding to key classes of reactions of atmospheric organics: functionalization (addition of polar functional groups), fragmentation (cleavage of C–C bonds) and oligomerization (covalent association of two organic species). The combination of these reaction types leads to complex movement through $\overline{OS}_C$–n_C space; however, the inevitable increase in $\overline{OS}_C$ with atmospheric oxidation implies that, given enough time, organics will generally move up and to the right (blue arrows), towards CO_2.

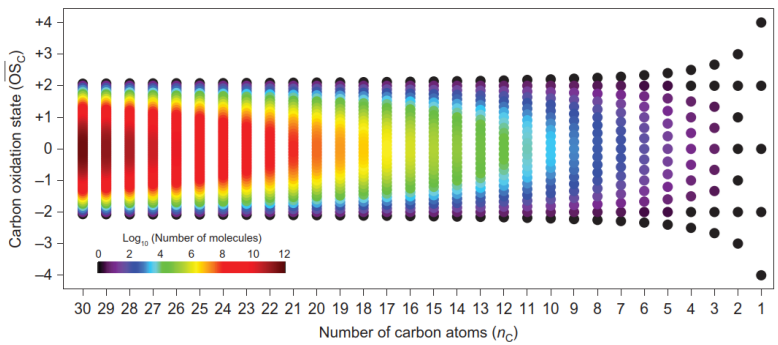

Figure 3 | Chemical complexity of organics as a function of oxidation state and carbon number. Points are coloured by the logarithm (base 10) of the number of possible compounds at a given $\overline{OS}_C$ and n_C, assuming an unbranched, acyclic carbon skeleton, and the addition of carbonyl, alcohol and acid groups only. Including a wider range of carbon skeletons or functional groups will lead to a dramatically steeper increase in chemical complexity with $\overline{OS}_C$ and n_C (ref. 31).

Kroll et al., *Nat. Chem.*, 2011

Comparison of oxidation reactions

	Combustion	Tropos. Ozone	SOA
Precursors	Hydrocarbons	VOCs	VOCs (larger)
Input	thermal energy	sunlight	sunlight
Oxidants		mostly radicals	
Products	CO, CO2, NOx, small molec.	O3, ROOH, carbonyls	larger molec.
Phase	gas	gas	gas + condensed

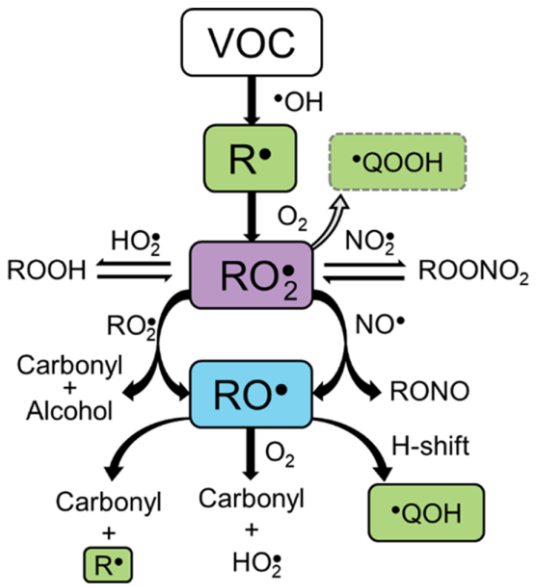

Figure 1. Canonical mechanism for the OH-initiated oxidation of a typical VOC in the troposphere, with a focus on the fates of the key organic radical intermediates along the reaction path: alkyl radicals (R, green), peroxy radicals (RO_2, purple), and alkoxy radicals (RO, blue). The QOOH formation pathway represents a recently appreciated mechanism that now ought to be considered part of the canonical atmospheric oxidation chemistry.

Barber et al., *J. Phys. Chem. A*, 2021

NO_x is a combustion biproduct.

Anthropogenic NO_x on natural background chemistry:

- More catalyst for O_3 formation
- Competes for oxidants forming highly oxidized, condensable products
- Precursor to oxidant (NO_3), organonitrate aerosol formation, inorganic nitrate formation

Examples of organic precursor compounds and their oxidation products

TABLE 14.13 Secondary Organic Aerosol Precursors and Aerosol Products[a]

Precursor	Major Products[b]		
			
α-Pinene	Pinonic acid	Pinic acid	Pinonaldehyde
	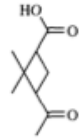		
β-Pinene	Norpinonic acid	Pinic acid	3-Oxo-pina ketone
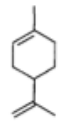	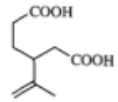	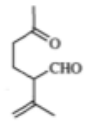	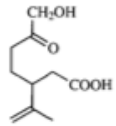
Limonene	Limonic acid	Limonaldehyde	7-Hydroxylimonic acid
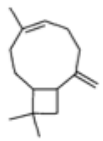	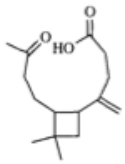	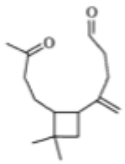	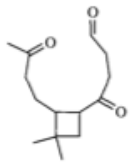
β-Carophyllene	β-Carophyllonic acid	β-Carophyllon aldehyde	Keto-β-carophyllon aldehyde
		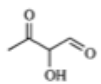	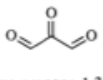
Toluene	Methyl glyoxal	2-Hydroxy-3-oxo butanal	2-Oxo propane-1,3-dial
	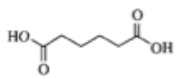	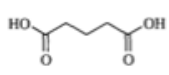	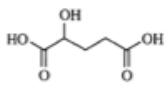
Cyclohexene	Adipic acid	Glutaric acid	2-Hydroxyglutaric acid

[a]Vertices represent carbon atoms and bonds between carbon atoms are shown. Hydrogen atoms bonded to carbons are not explicitly indicated. Stereochemistry is omitted for simplicity.
[b]A sampling of products are listed here; actual product distribution depends on oxidant type and concentration, precursor concentration, and atmospheric conditions.

Seinfeld and Pandis, 2006

Aerosol water

Water can also partition between vapor and aerosol phases. Aerosol water content is dependent on particle composition and ambient relative humidity (RH), and affects:

- gas/particle partitioning of other species
  - water is a solvent
  - removal rates of substances from the atmosphere–aerosol/gas lifetimes are different.
- particle size, which affects direct radiative forcing (light extinction)
- heterogeneous reaction rates (e.g., $N_2O_{5(g)} + H_2O_{(aq)} \rightleftharpoons 2HNO_{3(aq)}$)

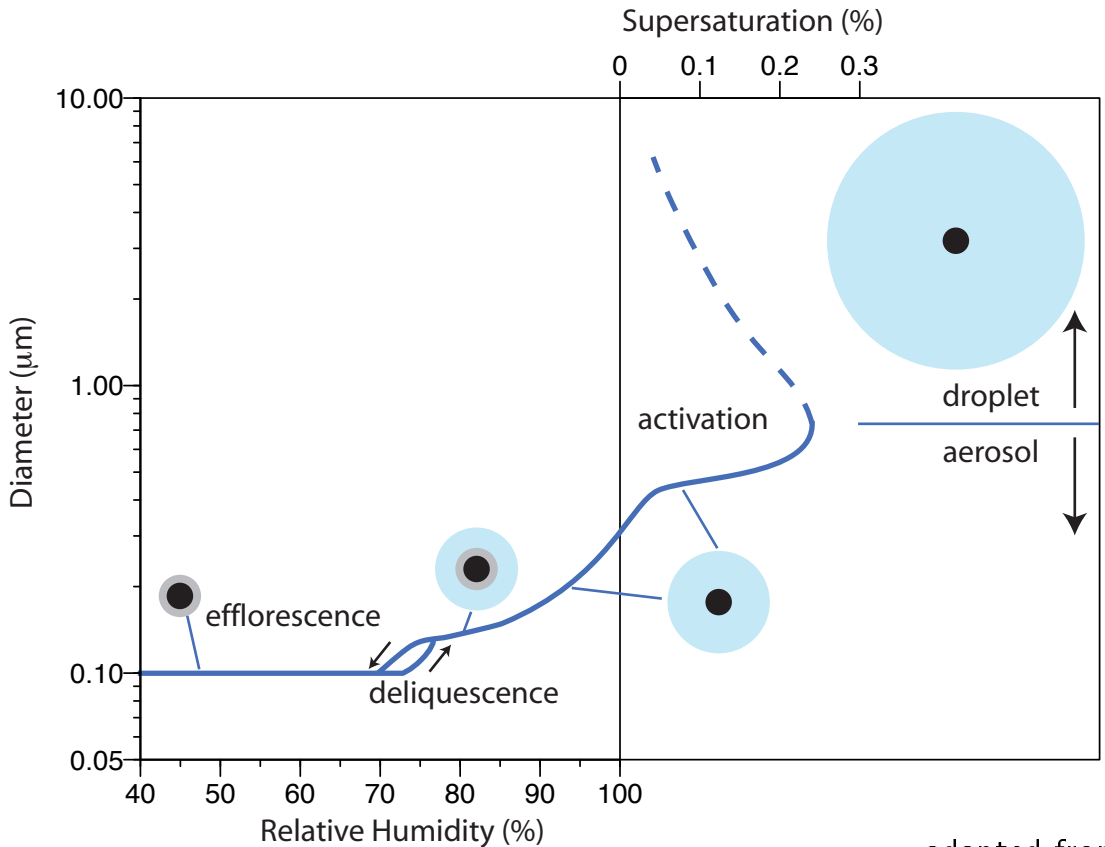

adapted from Pandis et al., 1995

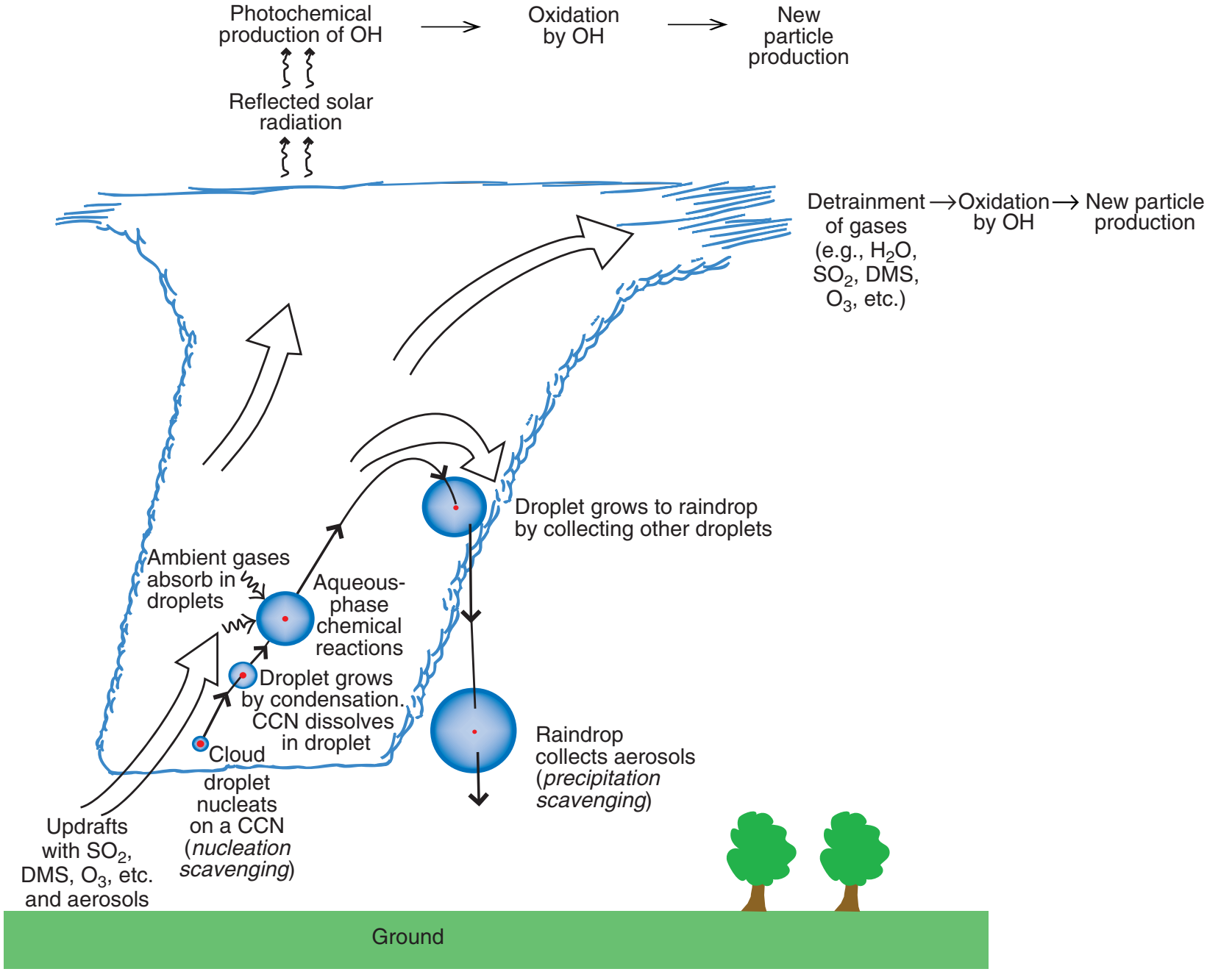

Wallace and Hobbs, 2006

Nitrate aerosols

Nitrate aerosols are expected to increase in the future due to increased emissions.

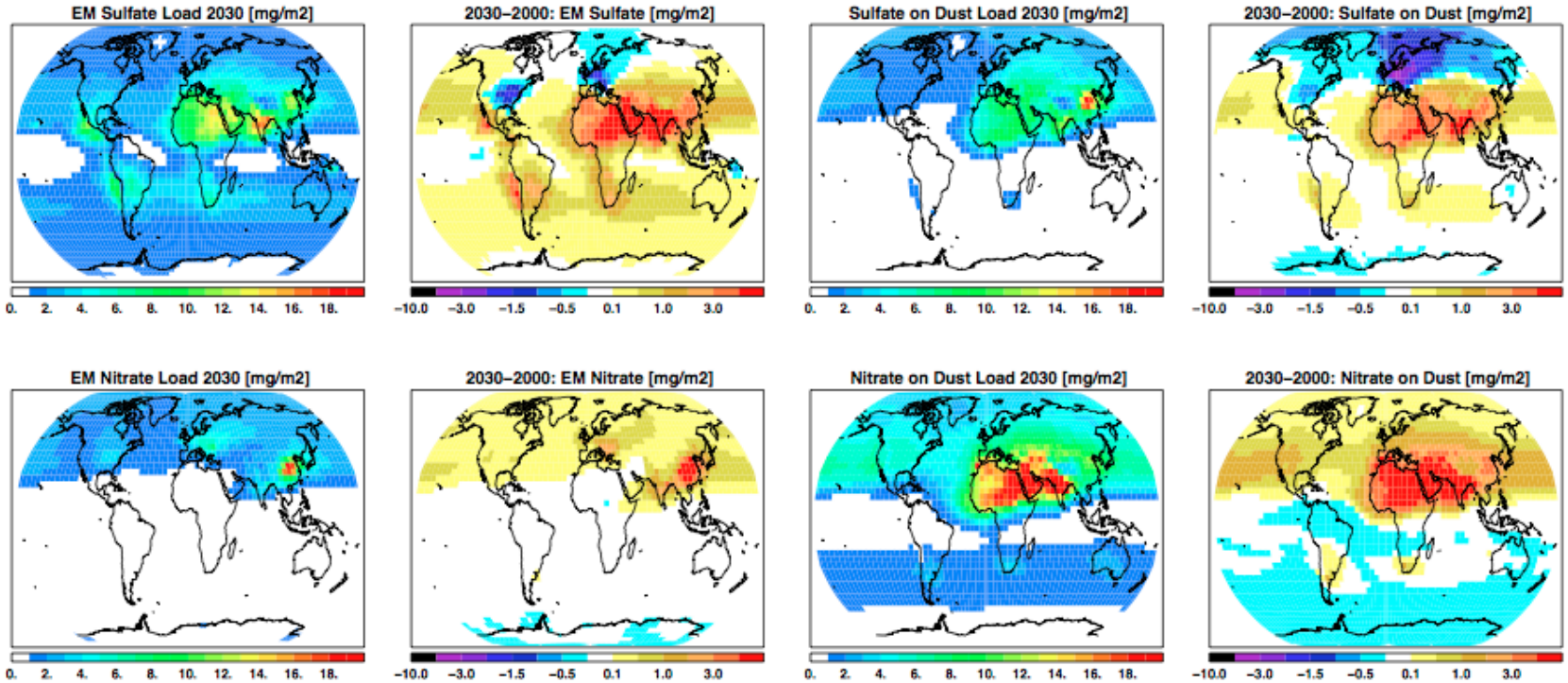

Fig. 8. Annual mean total column load for sulphate and nitrate aerosols of the year 2000, and the differences between 2030-2000. The first two maps show the externally mixed (EM), fine mode, sulphate contribution and the following two maps the coarse mode sulphate mass that is mixed with mineral dust. The second row shows the same maps but for nitrate aerosol. Units are [mg/m^2]. Bauer et al., 2007

Aerosols and gases have different deposition velocities
$\Rightarrow$ *gas/particle partitioning can affect lifetimes, atmospheric budget, and spatial distribution of semi-volatile species.*

Pittsburgh, PA 2001

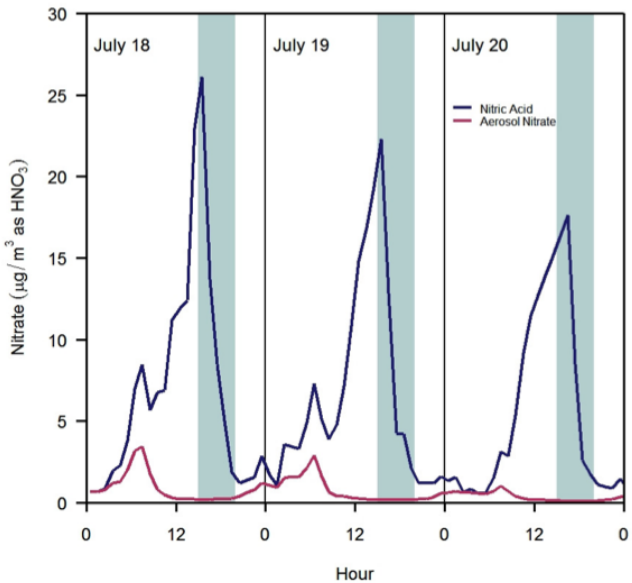

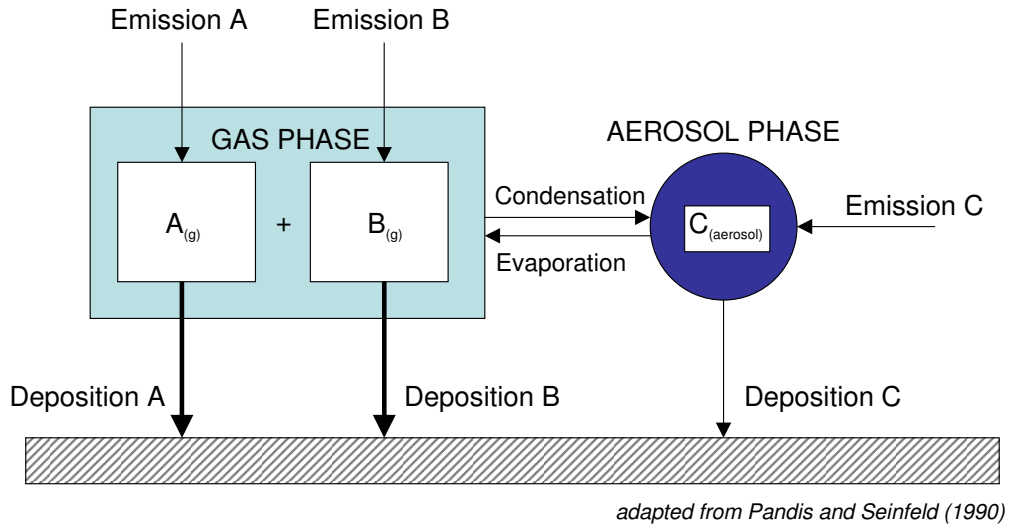

adapted from Pandis and Seinfeld (1990)

Example:

$$NH_{3(g)} + HNO_{3(g)} \rightleftharpoons NH_3NO_{3(s)}$$

Dynamics of mass transfer

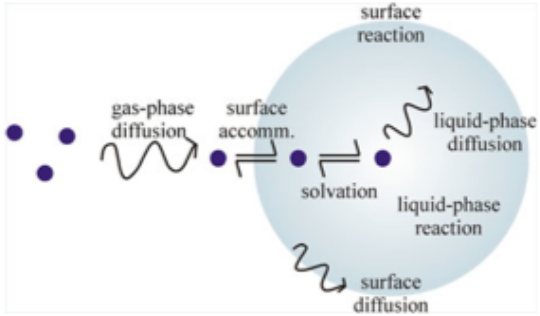

Fig. 2.5 Range of processes involved in uptake of a gas-phase species by a liquid aerosol particle

Knox, 2011

The molecular flux J to a particle is proportional to the particle size R_p, gas-phase diffusivity D_g, and concentration gradient between the gas-phase concentration c_∞ and the equilibrium vapor concentration c_{eq} at the particle surface:

$$J \sim R_p D_g (c_\infty - c_{\text{eq}})$$

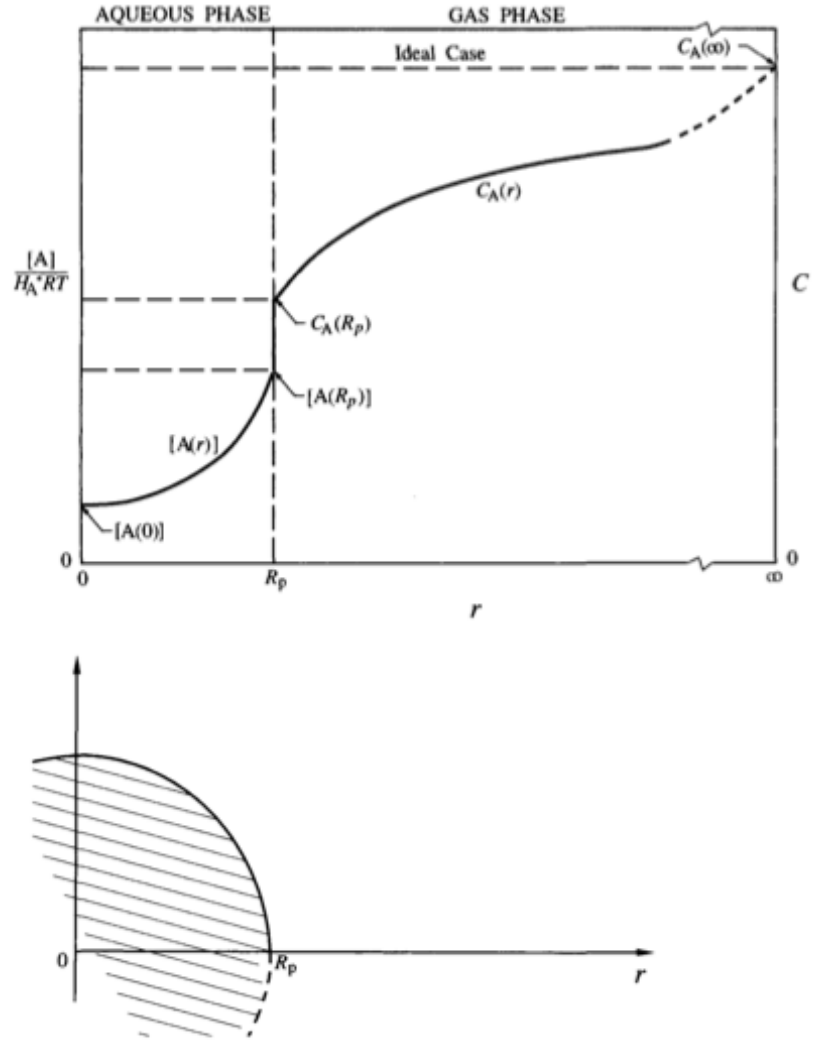

FIGURE 12.5 Schematic of gas- and aqueous-phase steady-state concentration profiles for the case where there are gas-phase, interfacial, and aqueous-phase mass transport limitations. Also shown is the ideal case where there are no mass transport limitations.

Seinfeld and Pandis, 2006

Studying phase equilibria

Assumption of equilibria (Wexler and Clegg, 2002):

- Calculations of aerosol composition and phase state often assume thermodynamic equilibrium.
- Thermodynamic equilibrium describes end point of all kinetic processes.
- Calculating the extent of a reaction or the concentration gradient driving molecular flux often require a knowledge of the thermodynamics.

Whether a system can be assumed to have achieved gas/particle equilibrium depends on the speed of this process (seconds to minutes in rapid cases; hours in other scenarios) relative to timescales of competing processes—e.g., emission, chemical production, and deposition.

Mass transfer limitations can introduce errors in partitioning predicted from equilibrium calculations under certain conditions [e.g., large particles (> 1 μm), low temperatures].

Example applications:

- partitioning of water
- partitioning of inorganic salts (solid and solutes in aqueous solution)
- partitioning of organics

Phase diagram for a pure substance in a closed system

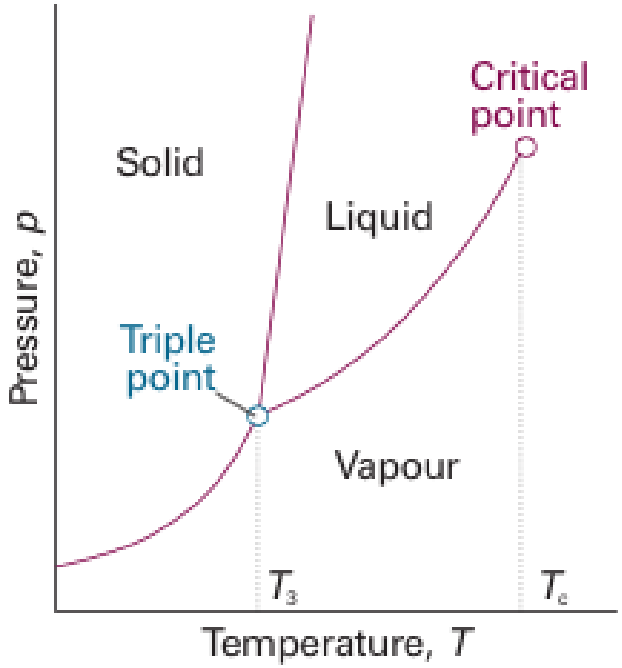

Fig. 4.1 The general regions of pressure and temperature where solid, liquid, or gas is stable (that is, has minimum molar Gibbs energy) are shown on this phase diagram. For example, the solid phase is the most stable phase at low temperatures and high pressures. In the following paragraphs we locate the precise boundaries between the regions.

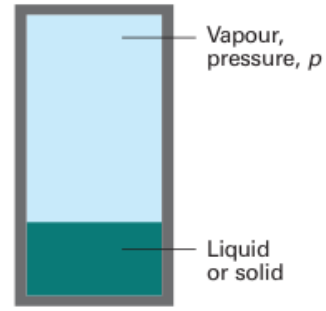

Fig. 4.2 The vapour pressure of a liquid or solid is the pressure exerted by the vapour in equilibrium with the condensed phase.

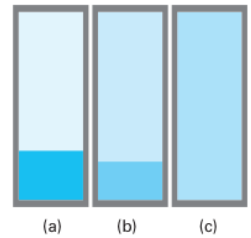

Fig. 4.3 (a) A liquid in equilibrium with its vapour. (b) When a liquid is heated in a sealed container, the density of the vapour phase increases and that of the liquid decreases slightly. There comes a stage, (c), at which the two densities are equal and the interface between the fluids disappears. This disappearance occurs at the critical temperature. The container needs to be strong: the critical temperature of water is 374°C and the vapour pressure is then 218 atm.

Akins and de Paula (2006)

Factors influencing pure component vapor pressures

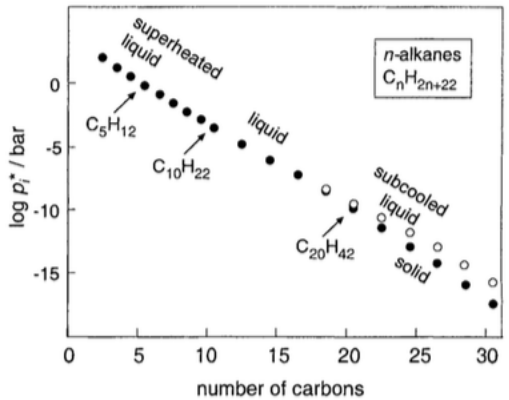

Figure 4.1 Vapor pressure at 25°C of *n*-alkanes as a function of chain length. The subcooled liquid vapor pressures have been calculated by extrapolation of p_{iL}^* values determined above the melting point (Eq. 4-8). Data from Daubert (1997) and Lide (1995).

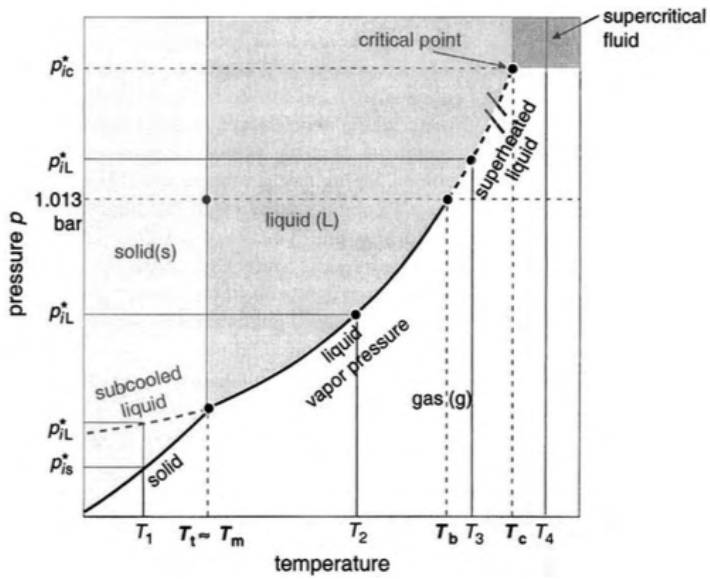

Figure 4.2 Simplified phase diagram of a pure organic chemical. Note that the boundary between the solid and liquid phase has been drawn assuming the chemical's melting point (T_m) equals its triple point (T_t), the temperature–pressure condition where all three phases coexist.) In reality, T_m is a little higher than T_t for some compounds and a little lower for others.

The pure component vapor pressure of a substance is dependent on molecular properties as well as their intermolecular forces:

- molecular size
- molecular shape (packing configuration)
- ionic interactions
- dispersion forces (dipole, van der Waals)

Environmental conditions:

- temperature

Schwarzenbach et al., 2003

Equilibrium vapor pressure

The equilibrium vapor pressure p_i for substance i determines the amount of substance that can be "held" in the gas phase at equilibrium.

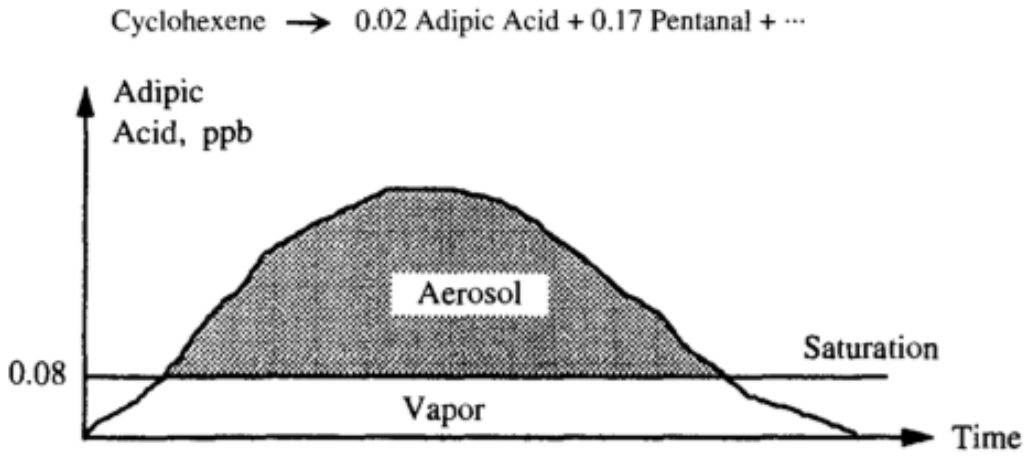

FIGURE 14.12 Schematic of the formation of secondary organic aerosol during the cyclohexene oxidation by mass transfer of adipic acid to the aerosol phase. This case corresponds to a single-component secondary organic aerosol phase without any interactions with the rest of the aerosol species.

Seinfeld and Pandis (2006)

p_i for a pure substance is the pure component vapor pressure ($p_i = p_i^*$). We will see how p_i can be derived for substances partitioned between the gas phase and liquid mixtures.

Mechanisms (driven by equilibrium vapor pressure).:

- *adsorptive* partitioning: solid and liquid surfaces
- *absorptive* partitioning: bulk aerosol solution

Absorptive mechanism shown to be predominant mechanism for atmospheric PM formation (since 1980s) in most scenarios.

How to relate composition x_i (mole fraction) to vapor pressure p_i?

A proportionality constant $\mathcal{R}$ can be defined for different ideal mixtures:

$$p_i = x_i \mathcal{R}$$

- ideal solution: $\mathcal{R}$ = pure component vapor pressure
- ideal-dilute solution: $\mathcal{R}$ = Henry's law coefficient

Two types of ideal mixtures

For substance i, let

- p_i = equilibrium vapor pressure
- x_i = mole fraction

"Ideal solution" (Raoult's law):

As $x_i \to 1$,

$$p_i = x_i p_i^*$$

where p_i^* = (possibly subcooled) pure-component liquid vapor pressure.

"Ideal-dilute solution" (Henry's law):

As $x_i \to 0$,

$$p_i = x_i K_{H,i}$$

where K_H = Henry's law constant.

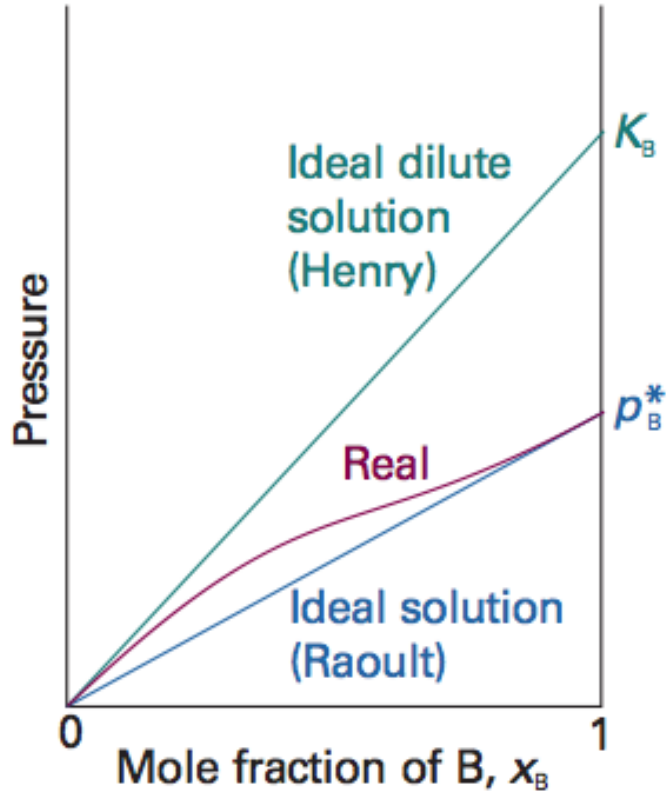

Fig. 5.15 When a component (the solvent) is nearly pure, it has a vapour pressure that is proportional to mole fraction with a slope p_B^* (Raoult's law). When it is the minor component (the solute) its vapour pressure is still proportional to the mole fraction, but the constant of proportionality is now K_B (Henry's law).

Atkins and de Paula, 2006

Ideal solutions

An expression for the equilibrium vapor pressure p_i^* can be derived from kinetic theory.

$$\text{rate of vaporization} = kx_i$$

$$\text{rate of condensation} = k' p_i$$

At equilibrium, these two rates are equal, which leads us to our intrepetation for p^*:

$$p_i = \frac{k}{k'} x_i \quad \Rightarrow \quad p_i^* = \frac{k}{k'}$$

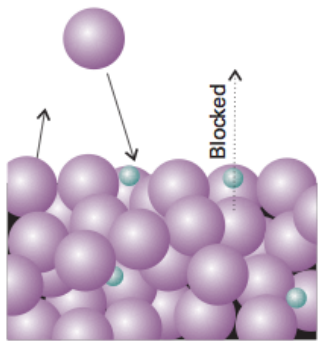

Fig. 5.13 A pictorial representation of the molecular basis of Raoult's law. The large spheres represent solvent molecules at the surface of a solution (the uppermost line of spheres), and the small spheres are solute molecules. The latter hinder the escape of solvent molecules into the vapour, but do not hinder their return.

Ideal-dilute solutions

Solute molecules in dilute solution are surrounded by solvent molecules; solute properties are therefore markedly different from pure components (unless solvent and solute molecules are structurally similar).

This leads to a proportionality constant between equilibrium vapor pressure p_i and solution composition x_i that is generally different from p_i^*.

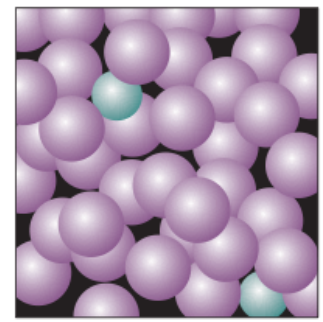

Fig. 5.16 In a dilute solution, the solvent molecules (the purple spheres) are in an environment that differs only slightly from that of the pure solvent. The solute particles, however, are in an environment totally unlike that of the pure solute.

Atkins and de Paula, 2006

Extending the framework to non-ideal solutions

Examples:

- ideal solution reference ($x_{\text{solvent}} \to 1$): water in cloud droplets, organic compounds
- ideal-dilute solution reference ($x_{\text{gas}} \to 0$): water-soluble gases dissolved in cloud droplets (e.g., CO_2, SO_2) and aerosols (e.g., HNO_3)

Aerosols are complex mixtures comprising many thousands of substances, and their G/P partitioning behavior is often non-ideal. We can characterize deviations from ideal states with an *activity coefficient*.

- Ideal solution:
$$p_i = \gamma_i^{I} x_i p_i^* \text{ where } \gamma_i^{I} \to 1 \text{ as } x_i \to 1.$$
- Ideal-dilute solution:
$$p_i = \gamma_i^{II} x_i p_i^* \text{ where } \gamma_i^{II} \to 1 \text{ as } x_i \to 0. \text{ Note that } \gamma^{II} = K_{H,i}/p_i^*.$$

Temperature dependence of vapor pressure

Clausius-Clapeyron equation:

$$\frac{d \ln p}{dT} = \frac{\Delta_{\text{vap}} H}{RT}$$

For small changes near p_0, T_0, $\Delta_{\text{vap}} H(T) \approx \Delta_{\text{vap}} H$:

$$\frac{p}{p_0} = \exp\left[\frac{-\Delta_{\text{vap}} H}{R}\left(\frac{1}{T} - \frac{1}{T_0}\right)\right]$$

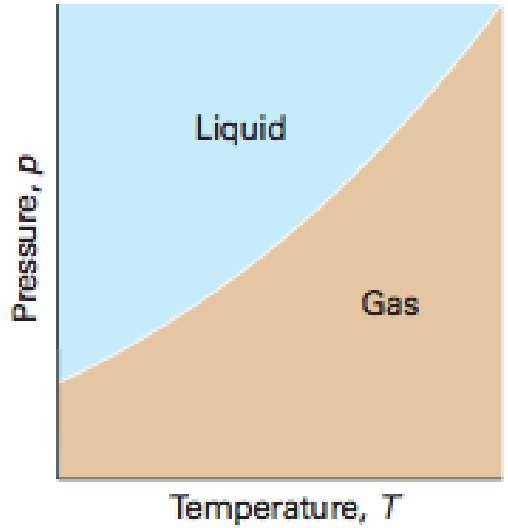

Fig. 4.14 A typical liquid–vapour phase boundary. The boundary can be regarded as a plot of the vapour pressure against the temperature. Note that, in some depictions of phase diagrams in which a logarithmic pressure scale is used, the phase boundary has the opposite curvature (see Fig. 4.7). This phase boundary terminates at the critical point (not shown).

Atkins and de Paula, *Physical Chemistry*, 2006

Deviations from ideality

For atmospheric aerosol solutions, intermolecular interactions in the condensed phase lead to additional energy exceeding that of its corresponding ideal solution.

- Thermodynamic properties of any pure substance are determined by intermolecular forces that operate on similar molecules.
- Thermodynamic properties of mixtures additionally depend on interactions between dissimilar molecules.
- Mixtures of real fluids do not form ideal solutions, although mixtures of similar liquids often exhibit behavior close to ideality.

Deviations from ideality are embodied the activity coefficient γ_i.

Examples of intermolecular forces:

- Electrostatic forces between charged ions, permanent dipoles (and multipoles).
- Induction forces between permanent dipole (or quadrupole) and an induced dipole.
- Dispersion and repulsion forces between nonpolar molecules.
- Chemical forces leading to association and solvation (e.g., hydrogen bonding)

Illustration: the force F between two molecules is related to the potential energy Γ by

$$F = -\frac{d\Gamma}{dr}$$

For an attractive potential, $-\Gamma(r)$ is the work which must be done to separate two molecules from the intermolecular distance r to infinite separation. (Forces of attraction are negative by convention.)

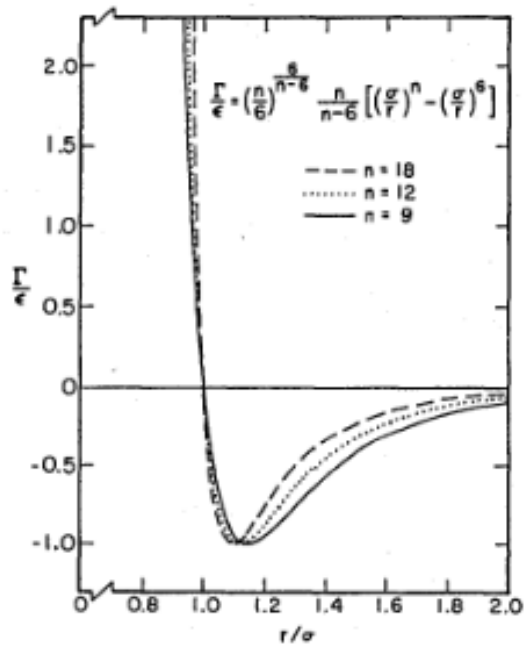

Figure 4-2 Three forms of Mie's potential for simple, nonpolar molecules.
Prausnitz et al., 1999

Mean activity coefficients in electrolyte solutions

Electrolytic dissociation of an electrically neutral electrolyte $M_{\nu+}X_{\nu-}$ in a high-dielectric-constant solvent (e.g., water) results in ν_+ cations and ν_- anions which have charges of z_+ and z_- respectively,

$$M_{\nu+}X_{\nu-} \rightleftharpoons \nu_+ M^{z+} + \nu_- X^{z-}$$

Electroneutrality imposes the constraint that the number of moles of the individual ionic species cannot be varied independently:

$$\nu_+ z_+ + \nu_- z_- = 0$$

For example, in the dissociation of sulfuric acid,

$$H_2SO_4 \rightleftharpoons 2H^+ + {SO_4}^{2-}$$

we have $\nu_+ = 2, z_+ = 1, \nu_- = 1, z_- = 2$.

There is no experimental way of separating the product $\gamma_+^{\nu+}\gamma_-^{\nu-}$ into contributions from the cations and anions. We can therefore introduce the mean activity coefficient,

$$\gamma_\pm = \left(\gamma_+^{\nu+}\gamma_-^{\nu-}\right)^{1/\nu} \quad \text{where } \nu = \nu_+ + \nu_-$$

Characterizing deviations from ideality with activity coefficients

Common activity coefficient models in environmental chemistry

Ionic strength (molar/molality scale)

$$I = \frac{1}{2} \sum_i m_i z_i^2$$

Debye-Hückel $I < 0.01$ M

$$\ln \gamma_i = -A z_i^2 I^{1/2}$$

Extended Debye-Hückel $I < 0.1$ M

$$\ln \gamma_i = -A \frac{z_i^2 I^{1/2}}{1 + a_i B I^{1/2}}$$

Davies (empirical extension to Debye-Hückel) $I < 0.5$ M

$$\ln \gamma_i = -A z_i^2 \left(\frac{I^{1/2}}{1 + I^{1/2}} - bI \right)$$

Typical ionic strengths in aquatic systems

- Freshwater: $I \approx 0.002$ M
- Seawater: $I \approx 0.7$ M
- Aerosols: $I = 6 - 30$ M (Nenes et al., 1998)

Aerosols require more sophisticated activity coefficient models than commonly used in other domains of environmental chemistry.

Activity coefficient models in chemical engineering

Many semi-empirical (i.e., fitted to data) parameterizations for γ_i begin with an expression for the excess molar Gibbs free energy g^E and deriving

$$RT \ln \gamma_i = \left(\frac{\partial n g^E}{\partial n_i} \right)$$

Example. two-suffix Margules equation:

$$g^E = A x_1 x_2$$

A is an empirical constant with units of energy.

Activity coefficients for components 1 and 2:

$$\ln \gamma_1 = \frac{A}{RT} x_2^2$$

$$\ln \gamma_2 = \frac{A}{RT} x_1^2$$

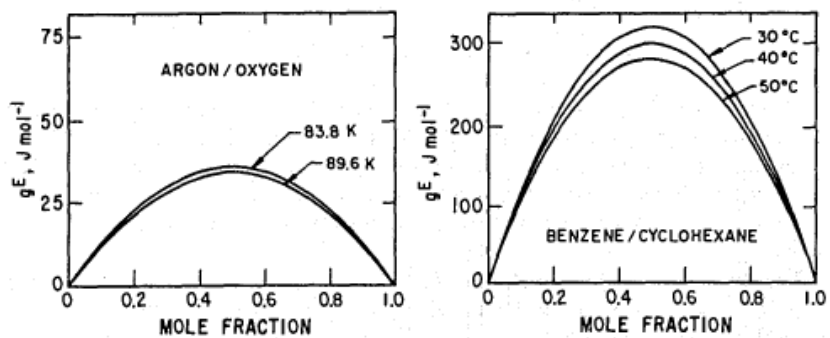

Figure 6-3 Applicability of two-suffix Margules equation to simple binary mixtures.

Prausnitz et al., 1999

Example activity coefficient model for electrolyte solutions used in aerosol chemistry

J. Phys. Chem. A **1998,** *102,* 2137−2154

Thermodynamic Model of the System H^+−NH_4^+−SO_4^{2-}−NO_3^-−H_2O at Tropospheric Temperatures

Simon L. Clegg* and Peter Brimblecombe
School of Environmental Sciences, University of East Anglia, Norwich NR4 7TJ, U.K.

Anthony S. Wexler
Department of Mechanical Engineering, University of Delaware, Newark, Delaware 19716

Received: September 17, 1997; In Final Form: December 2, 1997

$$\begin{aligned}\ln(f^*_{\pm}) = &- z_M z_X A_x[(2/\rho)\ln(1+\rho I_x^{1/2}) + \\ &I_x^{1/2}(1-2I_x/(z_M z_X))/(1+\rho I_x^{1/2})] + \\ &2z_M z_X x_1 B_{MX} g(\alpha_{MX} I_x^{1/2})/(z_M+z_X)^2 - x_M x_X B_{MX} \times \\ &[z_M z_X g(\alpha_{MX} I_x^{1/2})/(2I_x) + \exp(-\alpha_{MX} I_x^{1/2})(1 - z_M z_X/(2I_x))] + \\ &2z_M z_X x_1 B^1_{MX} g(\alpha^1_{MX} I_x^{1/2})/(z_M+z_X)^2 - x_M x_X B^1_{MX} \times \\ &[z_M z_X g(\alpha^1_{MX} I_x^{1/2})/(2I_x) + \exp(-\alpha^1_{MX} I_x^{1/2})(1 - z_M z_X/(2I_x))] + \\ &x_1(1-x_1)W_{1,MX} + 2x_1^2 x_1 U_{1,MX} + \\ &4x_1^2 x_1(2-3x_1)(z_M z_X/(z_M+z_X)^2)V_{1,MX} - W_{1,MX} \quad (14)\end{aligned}$$

State-of-the-art model used for simulating thermodynamic behavior of real organic aerosols; based on four-suffix Margules expansion.

For interactions of ions M and X,

- $f^*_{\pm}$ is the mean mole fraction activity coefficient of the ions
- x_1 mole fraction of the solvent; x_I total mole fractions of the ions
- I_x is the mole fraction ionic strength
- ρ a constant
- z_M and z_X are charge magnitudes
- A_x is the Debye-Hückel parameter
- B_{MX}, B^1_{MX}, α_{MX}, α^1_{MX} represent the extended Debye-Hückel function
- $W_{1,MX}$, $U_{1,MX}$, and $V_{1,MX}$ account for short-range interactions between the solvent (subscript 1) and ions.

Aerosol water

Aerosol hygroscopicity curve for various species. Notable characteristics:

- Growth factor (wet diameter over dry diameter), how much water the particle takes up
- deliquescence RH (DRH), the RH at which particle spontaneously takes up water
- efflorescence RH (ERH), the RH at which particle loses water (kinetically inhibited)

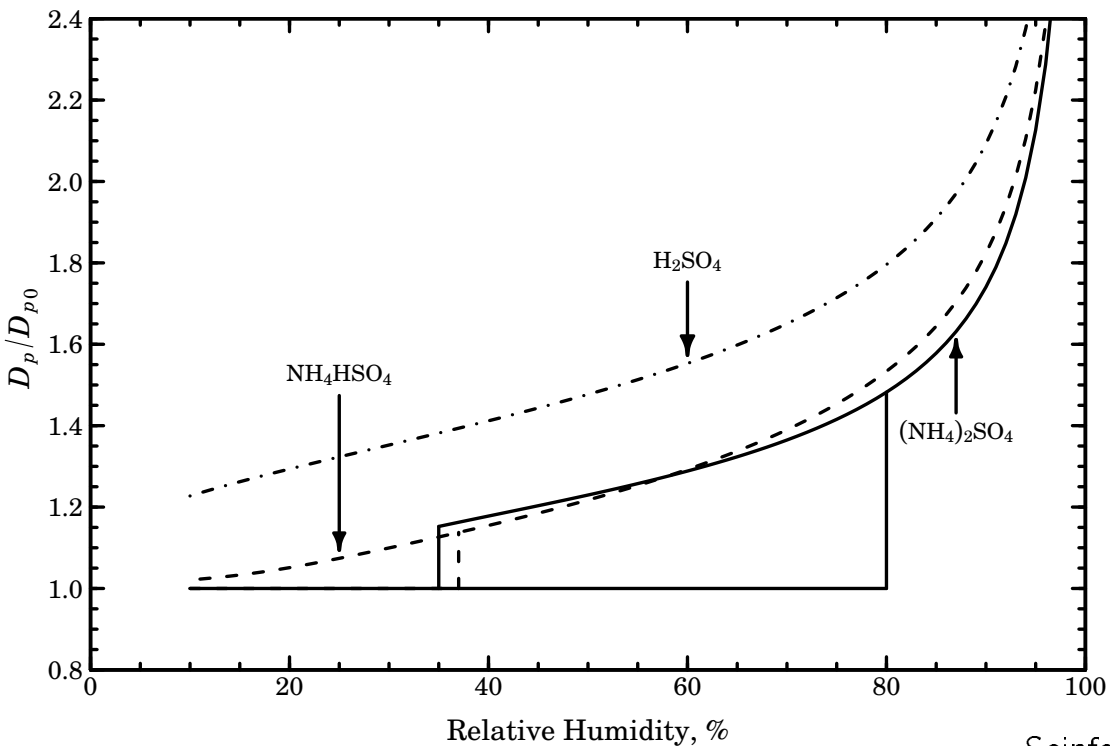

Seinfeld and Pandis, 2006

Deliquescence relative humidity (DRH)

As the RH is raised over the particle, deliquescence occurs when

- the RH equals the activity of water at saturation with respect to solute ("eutectic point" for multicomponent systems).
- the Gibbs free energy for the solution is lower than for the corresponding solid.

The RH at which this occurs is called the deliquescence relative humidity, abbreviated as DRH.

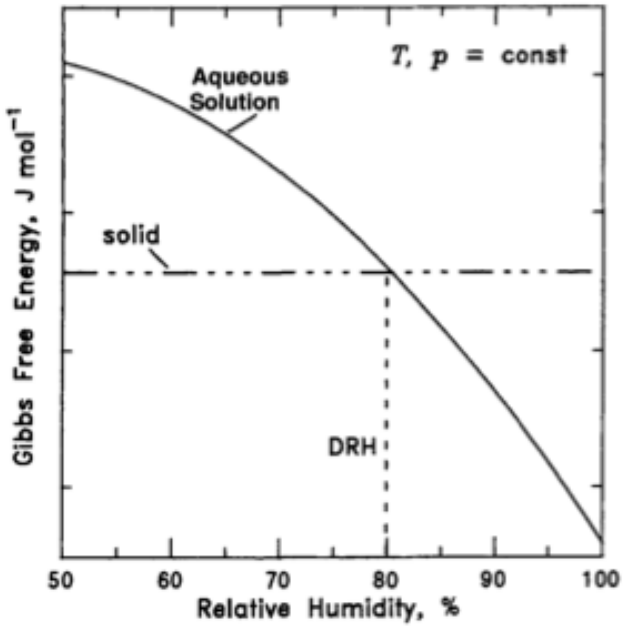

FIGURE 10.5 Gibbs free energy of a solid salt and its aqueous solution as a function of RH. At the DRH these energies become equal.

TABLE 10.1 Deliquescence Relative Humidities of Electrolyte Solutions at 298 K

Salt	DRH (%)
KCl	84.2 ± 0.3
Na_2SO_4	84.2 ± 0.4
NH_4Cl	80.0
$(NH_4)_2SO_4$	79.9 ± 0.5
NaCl	75.3 ± 0.1
$NaNO_3$	74.3 ± 0.4
$(NH_4)_3H(SO_4)_2$	69.0
NH_4NO_3	61.8
$NaHSO_4$	52.0
NH_4HSO_4	40.0

Sources: Tang (1980) and Tang and Munkelwitz (1993).

Seinfeld and Pandis, 2006

The water activity and temperature dependence of the DRH

Deliquescence relative humidity (DRH) is the water activity of the saturated solution of salt (mixture) at a given temperature

$$\frac{DRH(T)}{100} = a_w(T) \quad \text{at saturation}$$

The water activity over an approximately flat surface is

$$a_w(T) = \frac{p_w(T)}{p_w^0(T)} = \frac{RH}{100}$$

To derive the temperature dependence of the DRH, consider the following reactions:

$$H_2O_{(g)} \rightleftharpoons H_2O_{(aq)}$$

$$n\text{Solute}_{(s)} \overset{H_2O_{(aq)}}{\rightleftharpoons} n\text{Solute}_{(aq)}$$

- $\Delta_{sol}H$ (enthalpy of solution) describes the heat absorbed by the dissolution of the salt in this reaction
- n describes the number of moles of solute dissolved in water

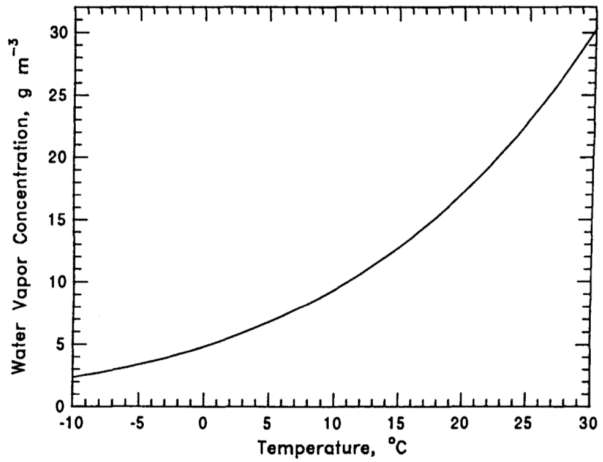

FIGURE 17.1 Saturation concentration of water over a flat water surface as a function of temperature. Values below 0°C correspond to supercooled (metastable) water.

Seinfeld and Pandis, 2006

Temperature-dependence of the DRH (from Clausius-Clapeyron):

$$\frac{d\ln(DRH/100)}{dT} = \frac{d\ln(p_w/p_w^0)}{dT} = -\frac{n\Delta_{sol}H}{RT^2}$$

The solubility n can be written as a polynomial in T and integrate $T_0 = 298$ K to T.

$$\ln \frac{DRH(T)}{DRH(T_0)} = \frac{\Delta_{sol} H}{R} \left[A \left(\frac{1}{T} - \frac{1}{T_0} \right) - B \ln \frac{T}{T_0} - C(T - T_0) \right]$$

TABLE 10.2 Solubility of Common Aerosol Salts in Water as a Function of Temperature ($n = A + BT + CT^2$, n = mol of solute per mol of water)

Salt	n (at 298 K)	A	B	C
$(NH_4)_2SO_4$	0.104	0.1149	-4.489×10^{-4}	1.385×10^{-6}
Na_2SO_4	0.065	0.3754	-1.763×10^{-3}	2.424×10^{-6}
$NaNO_3$	0.194	0.1868	-1.677×10^{-3}	5.714×10^{-6}
NH_4NO_3	0.475	4.298	-3.623×10^{-2}	7.853×10^{-5}
KCl	0.086	-0.2368	1.453×10^{-3}	-1.238×10^{-6}
NaCl	0.111	0.1805	-5.310×10^{-4}	9.965×10^{-7}

TABLE 10.3 Enthalpy of Solution for Common Aerosol Salts at 298 K

Salt	ΔH_s, kJ mol^{-1}
$(NH_4)_2SO_4$	6.32
Na_2SO_4	-9.76
$NaNO_3$	13.24
NH_4NO_3	16.27
KCl	15.34
NaCl	1.88

Seinfeld and Pandis, 2006

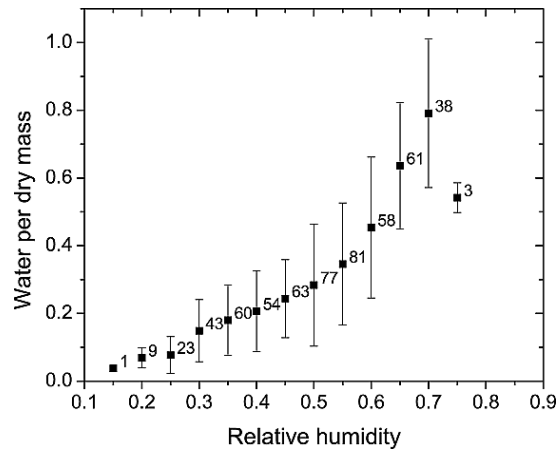

Mass of $PM_{2.5}$ aerosol bound water per $PM_{2.5}$ dry aerosol mass as a function of relative humidity during July 2001 [Pittsburgh, PA]. The error bars indicate the standard deviation, and the labels show the number of observations per each point.

Khlystov et al., *Aerosol Sci. Tech.*, 2005

Aerosol water content

Zadinski-Stokes-Robinson (1965) describe a way to estimate total liquid water content by summing contributions from each individual solute, assuming they are non-interacting.

For $m_{i,a}(a_w)$ and $m_{i,m}(a_w)$ are the molalities of solute i in (a) alone in solution and (m) in a mixture at a given water activity a_w, the ZSR relationship approximates that

$$\sum_i \frac{m_{i,m}(a_w)}{m_{i,a}(a_w)} = 1$$

Experimental data for $m_{i,a}$ and a_w are fitted to a polynomial expression of the form:

$$m_{i,a}(a_w) = Y_{0,i} + Y_{1,i}\,a_w + Y_{2,i}\,a_w^2 + \ldots$$

Multiplying both sides by c_w = liquid water content in air ($\mathrm{kg\,m^{-3}}$) and letting $\tilde{c}_i = m_{i,m}\,c_w$, the number of moles of i in air ($\mathrm{mol\,m^{-3}}$), we can get a more useable form of the equation:

$$c_w = \sum_i \frac{\tilde{c}_i}{m_{i,a}\,(a_w)}$$

Higher water content for aerosols at higher humidity (a_w) and solubility [$m(a_w)$].

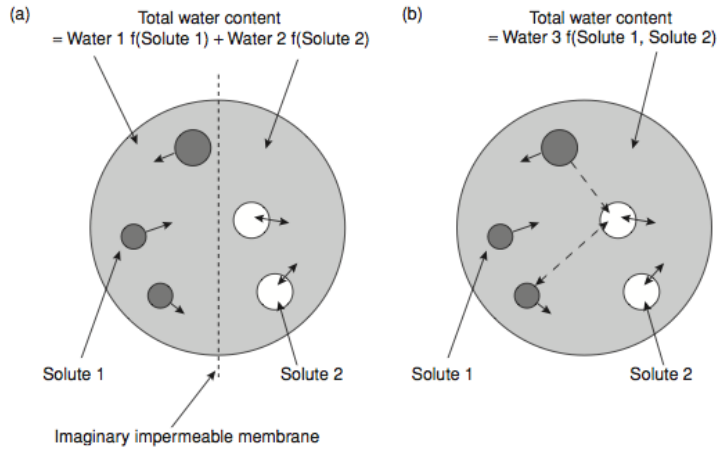

Figure 6.1 (a) Simple representation of the theory behind semi-ideality for a ternary aqueous system. Here the total water content is calculated by adding the individual contents from binary mixtures where the interactions between different solutes are neglected. (b) No ideality assumed. Here the interactions between different solutes are also taken into account. The solid arrows in the circle represent interactions between solute–solvent, whereas the dashed arrows represent interactions between the respective solutes.

Colbeck, 2008

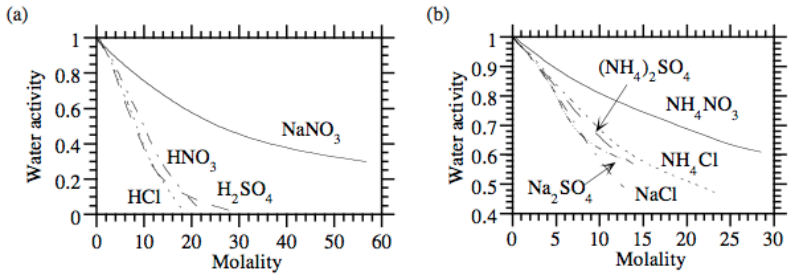

Figure 17.4 Water activity as a function of molality for several electrolytes at 298.15 K. The curves were obtained from (17.66) and the coefficients in Appendix Table B.10.

Jacobson, 2005

Ammonium nitrate formation

The dissociation constant (mixing ratio product):

$$K_p(T, RH) = \xi_{NH_3}\xi_{HNO_3} = 10^{18} p_{NH_3} p_{HNO_3}$$

Partial pressure p_i (e.g., atm) is related to the mixing ratio ξ_i (e.g., ppb) according to the relation,

$$\xi_i \text{ (ppb)} \approx 10^9 y_i = \frac{p_i}{p}$$

where y_i is the mole fraction in the gas phase.

K_p is defined in terms of equilibrium constant K_{AN} (activity of aerosol product over partial pressure of gas-phase reactants).

Solid-phase reaction:

$$NH_{3\,(g)} + HNO_{3\,(g)} \rightleftharpoons NH_4NO_{3\,(s)}$$

Aqueous-phase reaction:

$$NH_{3\,(g)} + HNO_{3\,(g)} \rightleftharpoons {NH_4}^+ + {NO_3}^-$$

Solid aerosol:

$$K_p = 10^{-18} K^{-1}_{AN(s)}(T)$$

Aqueous aerosol:

$$K_p = 10^{-18} K^{-1}_{AN(aq)}(T, RH)\, \gamma^2_{NH_4NO_3}\, x_{{NH_4}^+} x_{{NO_3}^-}$$

source: Wikimedia

Equlibrium constant

Equilibrium constant ($K_{\mathrm{AN(s)}}$ and $K_{\mathrm{AN(aq)}}$)

$$K = \exp\left(\frac{-\Delta_r G^{\circ}}{RT}\right)$$

Standard Gibbs free energy of reaction

$$\Delta_r G^{\circ} = \sum_i \nu_i \Delta_f G^{\circ}$$

where ν_i is the stoichiometric numbers for the reaction.

Solid ammonium nitrate:

$$\begin{aligned}\Delta_r G^{\circ} =& \Delta_f G^{\circ}_{\mathrm{NH_4NO_3(s)}} \\ &- \Delta_f G^{\circ}_{\mathrm{NH_3(g)}} - \Delta_f G^{\circ}_{\mathrm{HNO_3(g)}}\end{aligned}$$

Aqueous ammonium nitrate:

$$\begin{aligned}\Delta_r G^{\circ} =& - \Delta_f G^{\circ}_{\mathrm{NH_4{}^+(aq)}} - \Delta_f G^{\circ}_{\mathrm{NO_3{}^-(aq)}} \\ &- \Delta_f G^{\circ}_{\mathrm{NH_3(g)}} - \Delta_f G^{\circ}_{\mathrm{HNO_3(g)}}\end{aligned}$$

Temperature dependence of standard molar Gibbs free energy of the formation:

$$\begin{aligned}\Delta_f G^{\circ}(T) = T \Bigg[& \frac{\Delta_f G^{\circ}(T_0)}{T_0} \\ & + \Delta_f H^{\circ}(T_0)\left(\frac{1}{T} - \frac{1}{T_0}\right) \\ & + c_p(T_0)\left(\ln\frac{T_0}{T} - \frac{T_0}{T} + 1\right)\Bigg]\end{aligned}$$

where $\Delta_f G^{\circ}$ and $\Delta_f H^{\circ}$ are the standard molar free energy and enthalpy of formation, respectively. c_p is the molar constant-pressure heat capacity.

Thermochemical data

TABLE 4. Thermodynamic Parameters for Typical Atmospheric Aerosol Species[a]

Species	ΔG_f^o (kJ/mol)	ΔH_f^o (kJ/mol)	C_p^o (J/mol/K)
NaCl(s)	−384.138	−411.153	50.50
$NaNO_3$(s)	−367.00	−467.85	92.88
Na_2SO_4(s)	−1270.16	−1387.08	128.20
$NaHSO_4$(s)	−992.8	−1125.5	85[b]
NH_4Cl(s)	−202.87	−314.43	84.1
NH_4NO_3(s)	−183.87	−365.56	139.3
$(NH_4)_2SO_4$(s)	−901.67	−1180.85	187.49
NH_4HSO_4(s)	−823[c]	−1026.96	127.5[b]
$(NH_4)_3H(SO_4)_2$(s)	−1730[c]	−2207[c]	315[b]
HNO_3(g)	−74.72	−135.06	53.35
HCl(g)	−95.299	−92.307	29.126
NH_3(g)	−16.45	−46.11	35.06
H^+(aq)	0	0	0
Na^+(aq)	−261.905	−240.12	46.4
NH_4^+(aq)	−79.31	−132.51	79.9
HSO_4^-(aq)	−755.91	−887.34	−84.0
SO_4^{2-}(aq)	−744.53	−909.27	−293.0
NO_3^-(aq)[d]	−111.25	−207.36	−86.6
Cl^-(aq)	−131.228	−167.259	−136.4
OH^-(aq)	−157.244	−229.994	−148.5
NH_3(aq)	−26.50	−80.29	79.9[e]
H_2O(l)	−237.129	−285.830	75.291

[a] All values are from Wagman et al. (1982) except otherwise indicated.
[b] Wexler and Seinfeld (1991).
[c] Bassett and Seinfeld (1983).
[d] The values in Wagman et al. (1982) are in error; the equivalent values for HNO_3(aq) are listed instead.
[e] The value for NH_4^+ is listed.

Kim et al., *Aerosol Sci. Tech.*., 1993

Dependence of dissociation constant on temperature

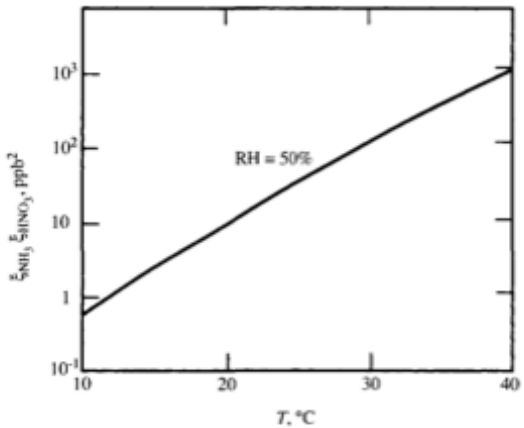

FIGURE 10.19 NH_4NO_3 equilibrium dissociation constant as a function of temperature at RH = 50%.

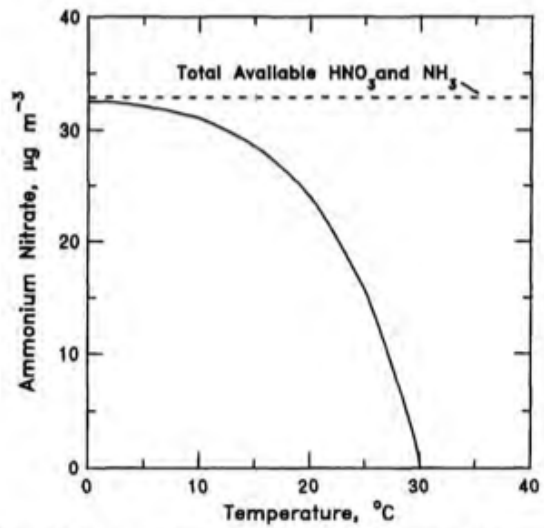

FIGURE 10.20 $NH_4NO_4(s)$ concentration as a function of temperature for a system containing 7 μg m^{-3} NH_3 and 26.5 μg m^{-3} HNO_3 at 30% RH. The difference between the total available mass (dashed line) and the NH_4NO_3 mass remains in the gas phase as $NH_3(g)$ and $HNO_3(g)$.

$K_p(T)$ is quite sensitive to temperature changes, varying over more than two orders of magnitude for typical ambient concentrations.

As $K_p(T)$ decreases with temperature, the gas-phase saturates at lower concentrations of vapor-phase HNO_3 and NH_3. The result is a higher fraction of total available HNO_3 and NH_3 condensing to the aerosol phase.

Seinfeld and Pandis, 2006

Dependence of dissociation constant on RH

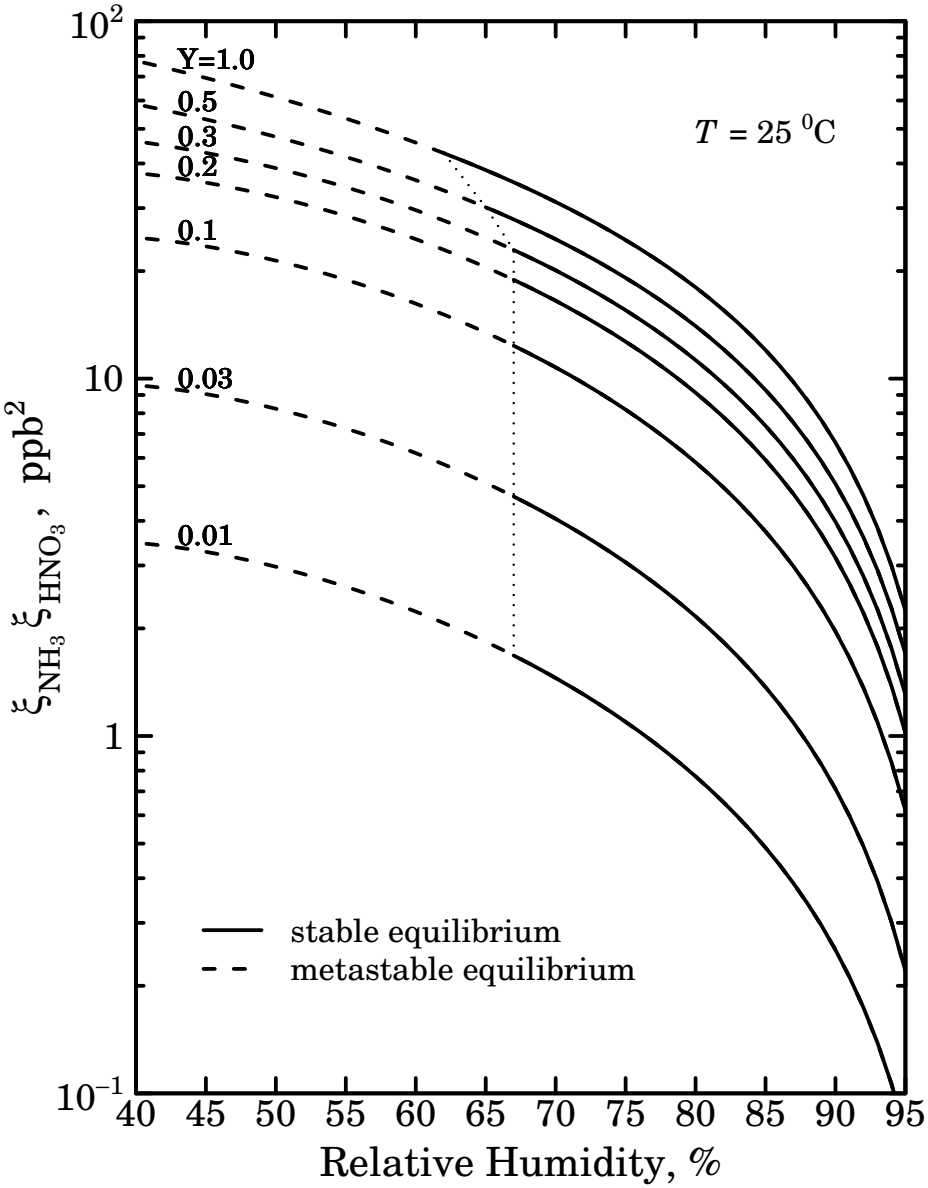

NH_4NO_3 equilibrium dissociation constant for an ammonium sulfate-nitrate solution as a function of relative humidity and ammonium nitrate ionic strength fraction defined by

$$Y = \frac{[NH_4NO_3]}{[NH_4NO_3] + 3[(NH_4)_2SO_4]}$$

at 298 K (Stelson and Seinfeld, 1982). Pure NH_4NO_3 corresonds to $Y = 1$.

From Seinfeld and Pandis 2006; calculations performed with E-AIM (Wexler and Clegg, *J. Geophys. Res.* , 2002; http://www.aim.env.uea.ac.uk/aim/aim.php)

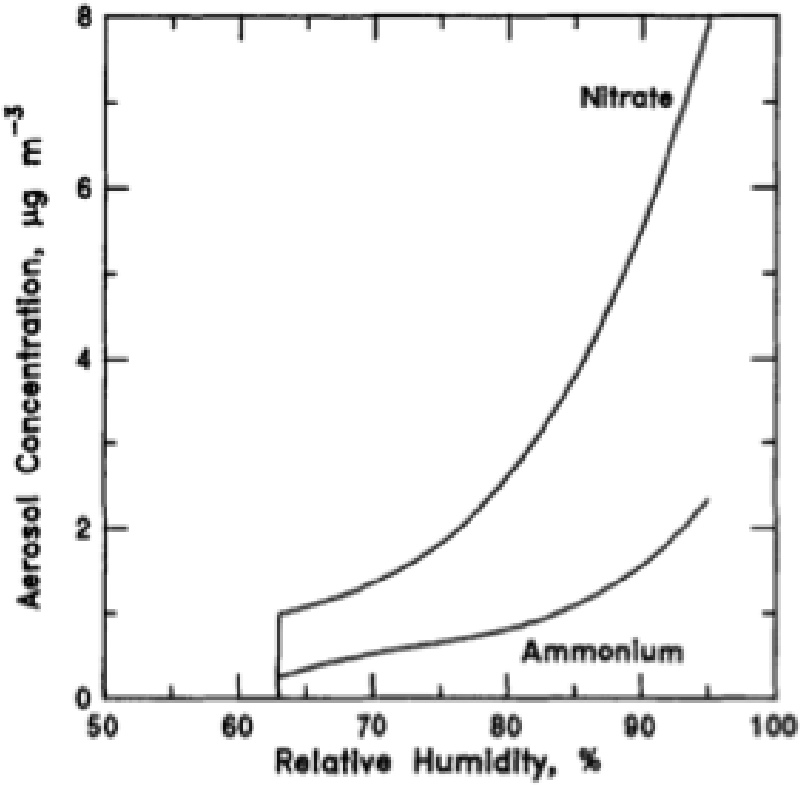

FIGURE 10.22 Calculated aerosol ammonium and nitrate concentrations as a function of relative humidity for an atmosphere with $[TA] = 5\,\mu g\,m^{-3}$, $[TN] = 10\,\mu g\,m^{-3}$, and $T = 300\,K$.

$K_p(T, RH)$ decreases with RH because there is more solvent to dissolve the NH_4^+ and NO_3^-; this results in more HNO_3 and NH_3 partitioned into the aerosol phase.

Seinfeld and Pandis, 2006

Use of thermodynamic models in emission control strategy evalaution

$$\frac{dPM}{d(SO_2 \text{ emissions})} = \frac{dPM}{d(\text{sulfate concentrations})} \frac{d(\text{sulfate concentrations})}{d(SO_2 \text{ emissions})}$$

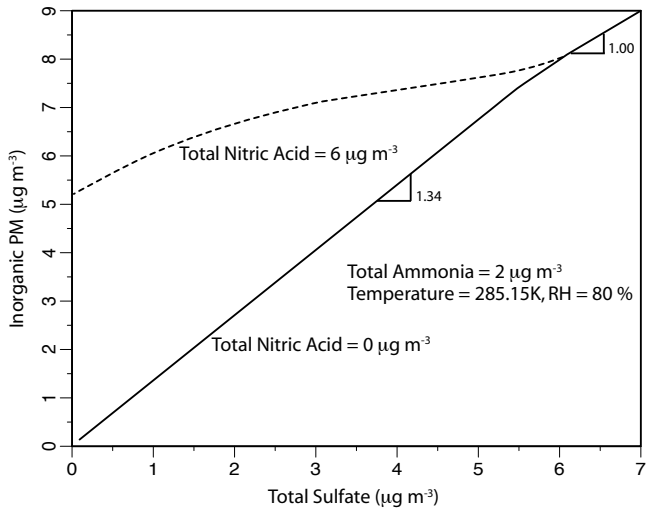

Ansari and Pandis, 1998

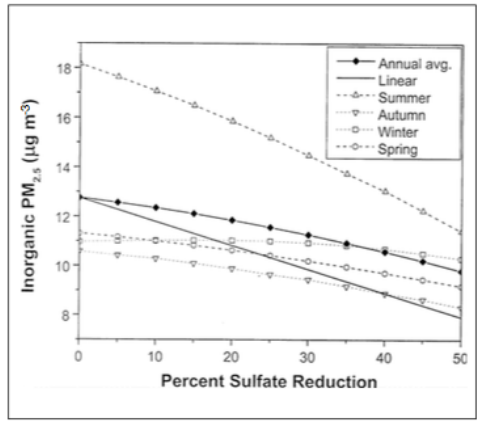

Figure 7. Modeled inorganic $PM_{2.5}$ at Brokensword as the sulfate concentration is reduced. The solid lines compare the equilibrium $PM_{2.5}$ response to the response if the system were assumed to respond linearly (Ψ_S = 1.35-μg $PM_{2.5}$ [μg H_2SO_4]$^{-1}$).

West et al., 1999

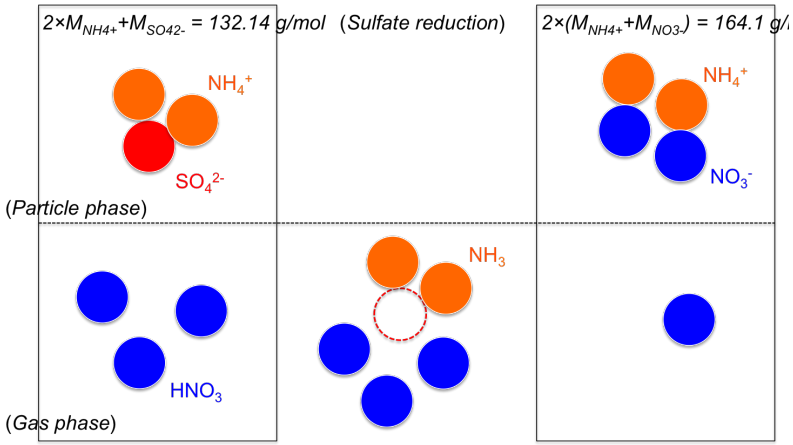

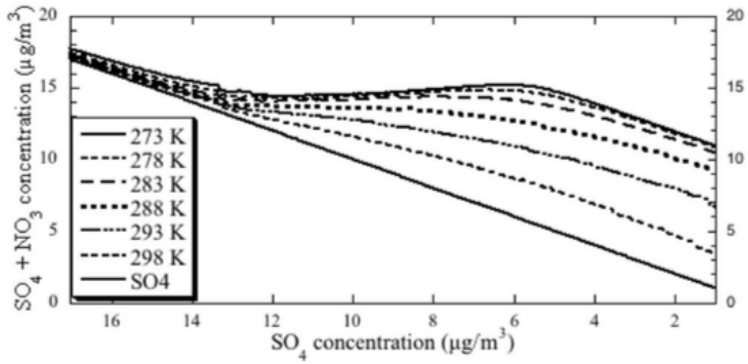

Fig. 1. The sum of nitrate and sulphate as function of the sulphate concentration at different temperatures for the following scenario: reflecting the constant ammonia and NO_x, total ammonia and total nitrate were chosen to be constant, 5 and 10 ug/m^3. The sulphate concentration was set to 22.5 ug/m^3 at the start and was gradually decreased. The relative humidity was set to 80%.

Erisman and Schaap, 2004

Organic aerosols

Effective saturation mass concentration

The bulk of organic matter mass in the atmosphere is assumed to *absorb* to a liquid organic phase rather than *adsorb* to the aerosol surface.

Ideal solution reference:

$$p_i = \gamma_i x_i p_i^0$$

where p_i^0 is the pure component vapor pressure of i in liquid.

Equilibrium ("saturation") concentrations of i in pure solution and in mixture:

$$C_i^0 = \frac{M_i}{RT} p_i^0$$

$$c_{g,i} = \frac{M_i}{RT} p_i$$

Mass fraction in particle phase:

$$X_{p,i} = \frac{c_{p,i}}{c_{p,i} + c_{g,i}} = \left(1 + \frac{c_{g,i}}{c_{p,i}}\right)^{-1} = \left(1 + \frac{C_i^*}{C_{OA}}\right)^{-1}$$

Organic aerosol concentration and effective saturation mass concentration:

$$C_{OA} = \sum_i c_{p,i} = \sum_i X_{p,i} \left(c_{p,i} + c_{g,i}\right)$$

$$C_i^* = \frac{\gamma_i C_i^0}{M_i / \overline{M}}$$

where $\overline{M}$ is the mean molecular weight of the organic aerosol.

γ_i is often assumed to be unity for lack of information (though models exist for its estimation).

Partitioning behavior

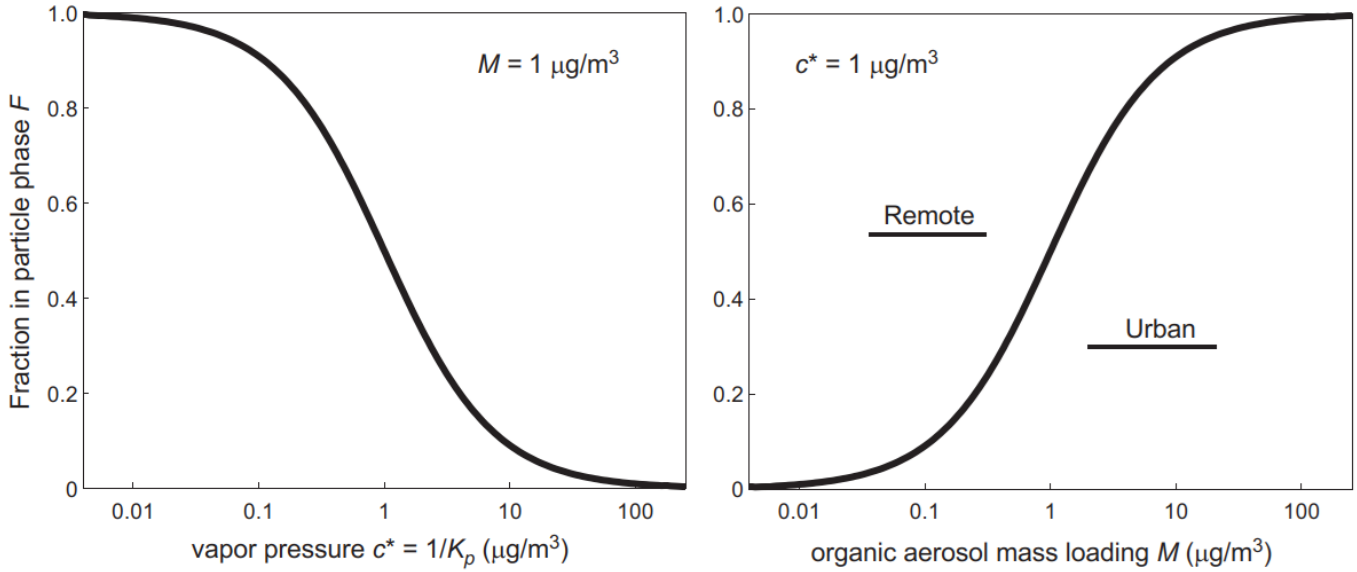

Fig. 1. Left panel: fraction F of a semivolatile compound in the particle phase as a function of its saturation mass concentration c^* ($= 1/K_p$), at an absorbing aerosol mass concentration $M = 1\,\mu g\,m^{-3}$. Right panel: particle fraction F as a function of M at $c^* = 1\,\mu g\,m^{-3}$. Approximate ranges of M values under remote and urban conditions are indicated.

Kroll and Seinfeld, *Atmos. Environ.*, 2008

Volatility basis set

- Typically don't know all molecular species i and their concentratons $c_{p,i}$
- Lumped species representation (represent all compounds with a few surrogate species of different volatility classes)
- Initially proposed: $C_i^* = \{10^{-2}, 10^{-1}, \ldots, 10^5\}\ \mu g\, m^{-3}$
- Find $c_{p,i}$ corresponding to each C_i^* through *perturbation* experiments: thermal analysis or isothermal dilution
- Use same basis set to represent mixtures from all sources additively in air quality models

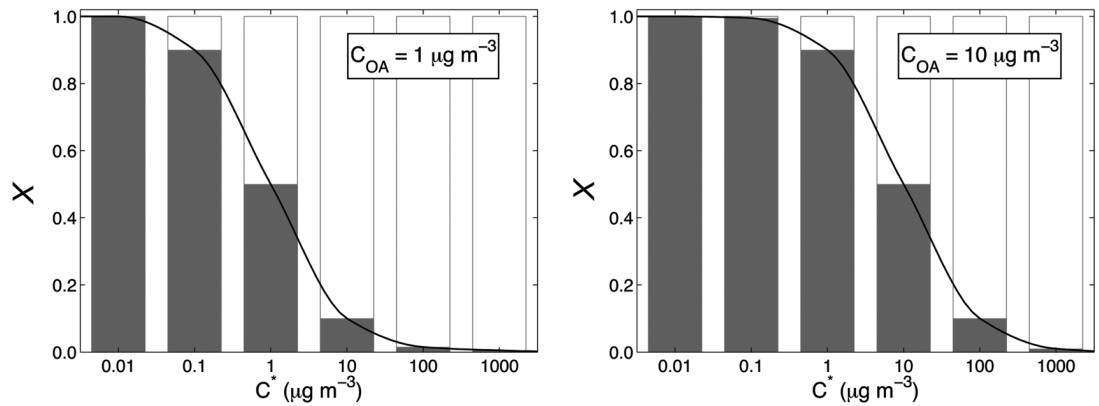

FIGURE 14.11 Fraction X_p of the total amount of a species in the aerosol phase as a function of C^* at two fixed values of C_{OA}: $1\,\mu g\,m^{-3}$ (left panel) and $10\,\mu g\,m^{-3}$ (right panel). In each case, $X_p = 0.5$ when $C^* = C_{OA}$.

Seinfeld and Pandis, 2016

Temperature dependence

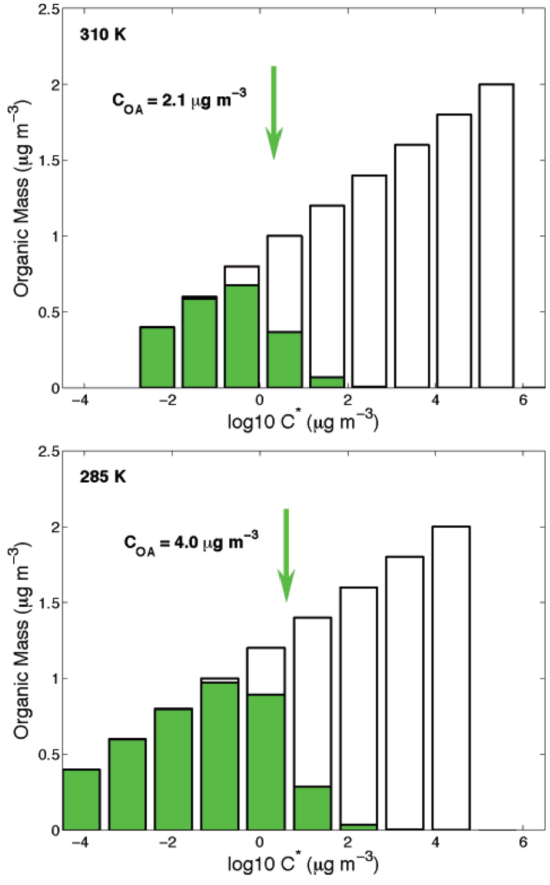

Volatility decreases as constituents are "aged" in the atmosphere (undergo photochemical transformations)

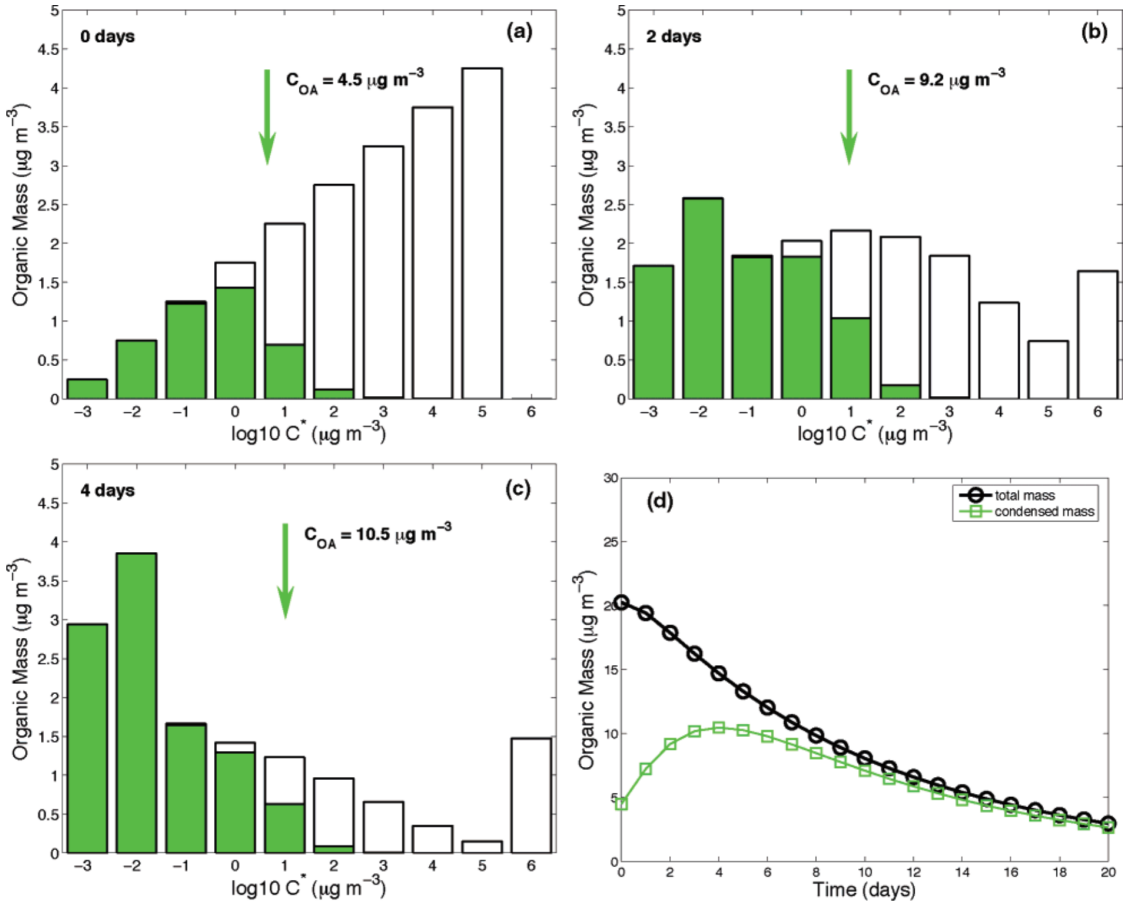

Donahue et al., *ES&T*, 2006

Competing effects

Temperature

- higher temperatures — faster reaction kinetics forming condensable products
- lower temperatures — lower volatility leading to condensation of reactoin products

Dilution

- cooling — favors condensation
- mixing leading to lower vapor concentrations — favors evaporation
- mixing leading to lower aerosol concentrations — favors evaporation

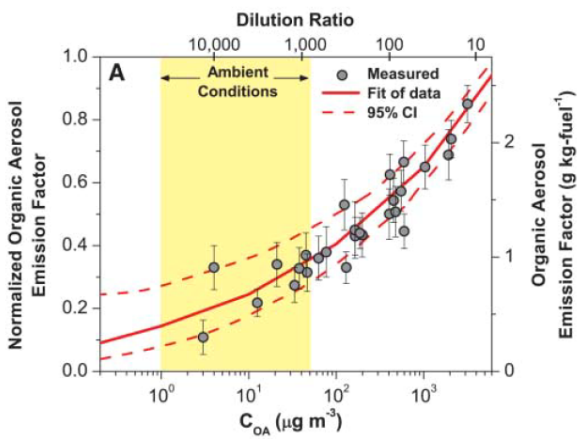

Robinson et al., *Science*, 2007

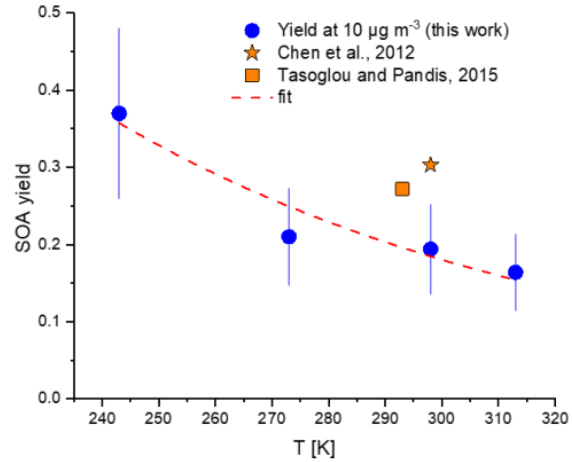

Figure 4. SOA mass yield from β-caryophyllene ozonolysis at a constant total organic aerosol mass (M_{org}) of 10 µg m^{-3} for temperatures between 243–313 K from this study in comparison with literature data. The dashed line represents a single exponential fit to the data. Chen et al. (2012) used OH/Cl scavenger and ammonium sulfate as seeds; Tasoglou and Pandis (2015) used OH/Cl scavenger. Another comparison with literature data is given in Fig. S6.

Gao et al., *Atmos. Chem. Phys.*, 2022

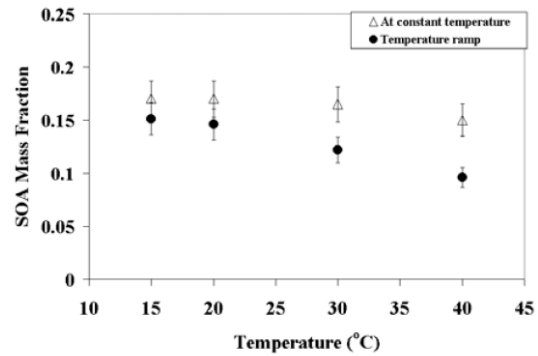

Figure 11. Comparison of α-pinene secondary organic average AMF measured for 38.3 ± 1.5 ppb α-pinene and 250 ppb ozone concentrations at constant temperature and secondary organic AMFs which were first obtained at 15°C and then later temperature ramp was carried out and secondary organic AMF were obtained at to 20°C, 30°C and 40°C.

Pathak et al., *Atmos. Environ.*, 2007

Mass closure

Do sum of measured chemical components add up to "total" gravimetric mass?

Sources of discrepancies:

- Possible retention of water
- Evaporative loss of semi-volatile substances
- Adsorption of additional gases to filter media or collected particles

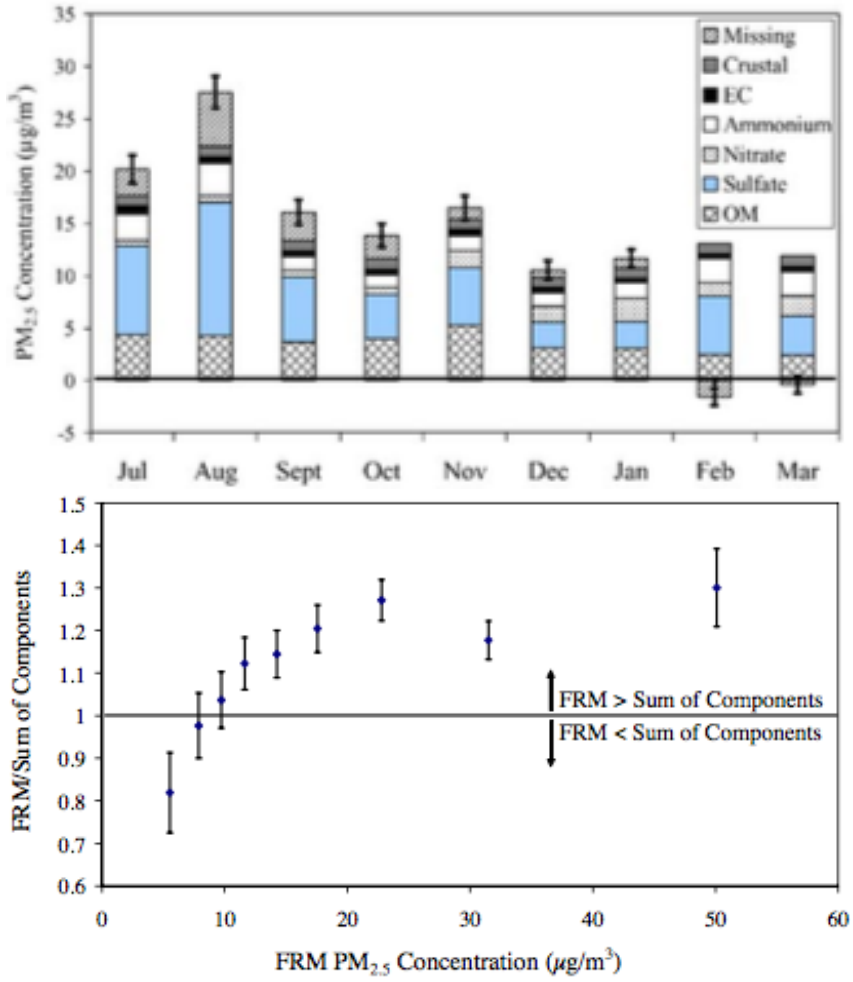

Rees et al., *Atmos. Environ.*, 2004

Selected bibliography

Atkins, P., and de Paula, J. *Physical Chemistry*. W. H. Freeman, 2006.

Denbigh, K. G. *The Principles of Chemical Equilibrium: With Applications in Chemistry and Chemical Engineering*. Cambridge University Press, 1981.

Hinchliffe, A. *Molecular Modelling for Beginners*. 2nd ed. Wiley, Hoboken, NJ, 2008.

Jacobson, M. Z., *Fundamentals of Atmospheric Modeling*. Cambridge University Press, Cambridge, 2005.

Lewis, G. N. and Randall, M., *Thermodynamics*. 2nd ed. McGraw Hill, 1961.

Leach, A. *Molecular Modelling: Principles and Applications*. 2nd ed. Harlow, England, Prentice Hall, New York, 2001.

Prausnitz, J. M., Lichtenthaler, R. N., and de Azevedo, E.G. *Molecular Thermodynamics of Fluid-Phase Equilibria*. Prentice Hall, Upper Saddle River, 1998.

Seinfeld, J. H. and Pandis, S. N. *Atmospheric Chemistry and Physics: From Air Pollution to Climate Change*. 3rd ed. John Wiley & Sons, New York, 2016.

Tester, J. W. and Modell, M. *Thermodynamics and Its Applications*. Prentice Hall, Upper Saddle River, 1997.

Tuckerman, M. E. *Statistical Mechanics: Theory and Molecular Simulation*. Oxford University Press, New York, 2010.